

PHYSICAL CHEMISTRY 2016

2<sup>nd</sup> International Meeting  
on

***Materials Science for  
Energy Related Applications***

**BOOK OF ABSTRACTS**

September 29-30, 2016

University of Belgrade - Faculty of Physical Chemistry, Belgrade

KTH  
ROYAL INSTITUTE OF TECHNOLOGY  
Stockholm, Sweden



UNIVERSITY OF BELGRADE  
FACULTY OF PHYSICAL CHEMISTRY  
Belgrade, Serbia



THE SOCIETY OF  
PHYSICAL CHEMISTS OF SERBIA  
Belgrade, Serbia





2<sup>nd</sup> International Meeting  
on  
**Materials Science for Energy Related Applications**

held on September 29-30, 2016 at the University of Belgrade, Faculty of Physical Chemistry,  
Belgrade, Serbia

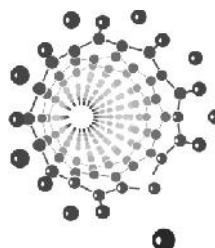
is a satellite event of  
**PHYSICAL CHEMISTRY 2016**  
*13<sup>th</sup> International Conference on Fundamental  
and Applied Aspects of Physical Chemistry*

organized by

**KTH**  
**ROYAL INSTITUTE OF**  
**TECHNOLOGY**  
**Stockholm, Sweden**



**UNIVERSITY OF BELGRADE**  
**FACULTY OF PHYSICAL**  
**CHEMISTRY**  
**Belgrade, Serbia**



in co-operation with  
**THE SOCIETY OF PHYSICAL CHEMISTS OF SERBIA**



*Funded by*  
**Swedish Research Council**

### **Scientific Committee**

N. V. Skorodumova, KTH, Stockholm, Sweden

B. Johansson, KTH, Stockholm, Sweden

I. Pašti, University of Belgrade, Faculty of Physical Chemistry, Serbia

A. Ruban, KTH, Stockholm, Sweden

R. Compton, University of Oxford, United Kingdom

S. Mentus, University of Belgrade, Faculty of Physical Chemistry, Serbia

A. Kokalj, Jožef Stefan Institute, Slovenia

G. Ćirić-Marjanović, University of Belgrade, Faculty of Physical Chemistry, Serbia

M. Gaberšček, National Institute of Chemistry, Slovenia

### **Organizing Committee**

B. Šljukić Paunković, University of Belgrade, Faculty of Physical Chemistry, Serbia

N. Gavrilov, University of Belgrade, Faculty of Physical Chemistry, Serbia

A. Dobrota, University of Belgrade, Faculty of Physical Chemistry, Serbia

M. Baljžević, Paul Scherrer Institute, Switzerland

A. Marković, University of Oldenburg, Germany

K. Batalović, University of Belgrade, Vinča Institute, Serbia

PHYSICAL CHEMISTRY 2016

*13<sup>th</sup> International Conference on Fundamental  
and Applied Aspects of Physical Chemistry*

2<sup>nd</sup> International Meeting

# **MATERIALS SCIENCE FOR ENERGY RELATED APPLICATIONS**

September 29-30, 2016, University of Belgrade – Faculty of Physical Chemistry,  
Belgrade, Serbia

**BOOK OF ABSTRACTS**

BELGRADE, SERBIA 2016



2<sup>nd</sup> International Meeting  
on  
***Materials Science for Energy Related Applications***

**BOOK OF ABSTRACTS**

**Editors**

Prof. Dr. Natalia V. Skorodumova

Dr. Igor A. Pašti

**Publisher**

UNIVERSITY OF BELGRADE – FACULTY OF PHYSICAL CHEMISTRY  
Belgrade, Serbia

**For the Publisher**

Prof. Dr. Gordana Irić-Marjanović

Printed by

Knjigoveznica Stevanović, Belgrade

Print run

75 copies

ISBN 978-86-82139-62-1

BELGRADE, SERBIA 2016

CIP -

66.017/.018(048)  
621.315:66.017(048)  
544.47(048)

INTERNATIONAL Meeting on Materials Science for Energy Related Applications  
(2 ; 2016 ; Beograd)

Book of Abstracts / 2nd International Meeting [on] Materials Science for Energy Related Applications, September 29-30, 2016, Belgrade, Serbia [within] 13th International Conference on Fundamental and Applied Aspects of Physical Chemistry - Physical Chemistry 2016 ; [organized by KTH Royal Institute of Technology, Stockholm, Sweden [and] University of Belgrade, Faculty of Physical Chemistry, Belgrade [and] the Society of Physical Chemistry of Serbia, Belgrade ; Natalia V. Skorodumova, Igor A. Pašti]. - Belgrade : Faculty of Physical Chemistry, 2016 (Belgrade : Knjigoveynica Stevanovi ). - 84 str. : ilustr. ; 29 cm

Tiraž 75. - Bibliografija uz svaki apstrakt.

ISBN 978-86-82139-62-1

1. International Conference on Fundamental and Applied Aspects of Physical Chemistry (13 ; 2016 ; Beograd) 2. Royal Institute of Technology (Štokholm)

a) - b) -  
c) -

COBISS.SR-ID 225930764



# T A B L E O F C O N T E N T

<b>Plenary lectures</b>	
<u>Aleksandra Dapčević</u> <i>LANTHANOIDE DOPED <math>\delta</math>-Bi<sub>2</sub>O<sub>3</sub> WITH ENHANCED CONDUCTIVITY</i>	1
<u>Chris Batchelor-McAuley</u> <i>HYDROGEN OXIDATION: FROM THERMODYNAMICS TO THE REACTION KINETICS AT SINGLE NANOPARTICLES</i>	3
<b>Solid electrolytes and oxide materials for energy related applications</b>	
V. Lutsyk, A. Zelenaya, <u>M. Parfenova</u> <i>CRYSTALLIZATION PATHS IN CERAMIC SYSTEMS WITH THE MATERIALS FOR ENERGY APPLICATION</i>	5
<u>A.Radojković</u> , M. Žunić, S.Savić, Z. Branković, G. Branković <i>CHEMICAL STABILITY OF DOPED BaCe<sub>0.9</sub>Y<sub>0.1</sub>O<sub>3-<math>\delta</math></sub> AS A PROTON CONDUCTING ELECTROLYTE FOR IT-SOFC</i>	7
<u>Olga Yu. Vekilova</u> , Johan O. Nilsson, Johan Klarbring, Sergei I. Simak, Natalia V. Skorodumova <i>IONIC CONDUCTIVITY IN DOPED CERIA FROM AB INITIO NON-EQUILIBRIUM MOLECULAR DYNAMICS COMBINED WITH A COLOR-DIFFUSION ALGORITHM</i>	9
<u>Johan O. Nilsson</u> , Mikael Leetmaa, Olga Yu. Vekilova, Sergei I. Simak, Natalia V. Skorodumova <i>SIMULATION OF ION CONDUCTIVITY IN DOPED CERIA FROM FIRST PRINCIPLES</i>	10
<u>Sanja Pršić</u> , Slavica M. Savić, Zorica Branković, Stanislav Vrtnik, Slavko Bernik and Goran Branković, <i>THERMOELECTRIC PROPERTIES OF NaCo<sub>2-x</sub>Cu<sub>x</sub>O<sub>4</sub> (x = 0, 0.01, 0.03, 0.05) CERAMIC</i>	11

## Heterogeneous catalysis and Photocatalysis

Ivana Lukić, Željka Kesić, Miodrag Zdujić, Dejan Skala

*SYNTHESIS OF METAL GLYCEROLATES AS CATALYSTS FOR BIODIESEL  
PRODUCTION*

13

Jovana Ćirković, Danijela Luković Golić, Aleksandar Radojković,

Aleksandra Dapčević, Zorica Branković, Goran Branković

*PHOTOCATALYTIC PROPERTIES OF BiFeO<sub>3</sub> PARTICLES SYNTHESIZED BY  
ULTRASOUND SOL-GEL ASSISTED ROUTE*

14

T. D. Savić, M. I. Čomor, I. A. Janković, D. Ž. Veljković, S. D. Zarić

*SURFACE MODIFICATION OF ANATASE NANOPARTICLES MODIFIED WITH  
CATECHOLATE TYPE LIGANDS: EXPERIMENTAL AND DFT STUDY OF  
OPTICAL PROPERTIES*

15

Anton Kokalj

*A MODEL STUDY OF METHANE DEHYDROGENATION ON Rh@Cu(111)*

16

Vesna Đorđević, Jasmina Dostanić, Davor Lončarević, S. Phillip Ahrenkiel,

Dušan N. Sredojević, Nenad Švrakić, Jovan M. Nedeljković

*VISIBLE-LIGHT RESPONSIVE Al<sub>2</sub>O<sub>3</sub> PARTICLES*

18

Nikola Tasić, Zorica Marinković Stanojević, Zorica Branković,

Uroš Lačnjevac, Milan Žunić, Martina Gilić, Goran Branković

*NANOSIZED ANATASE PARTICLES FOR APPLICATION IN DYE-SENSITIZED  
SOLAR CELLS (DSSCs)*

19

Nikola Bilišković, Danijela Vojta

*IN-SITU TEMPERATURE DEPENDENT INFRARED SPECTROSCOPY OF  
AMMONIA BORANE DEHYDROGENATION*

20

## Surface processes

Aleksandar Z. Jovanović

*THEORETICAL ANALYSIS OF ADSORPTION PROPERTIES OF DOPED  
HEXAGONAL MgO NANOTUBES*

21

<u>Igor A. Pašti</u> , Natalia V. Skorodumova	
<i>CHANGING REACTIVITY OF SUPPORTED METAL ATOMS BY SUBSTRATE DOPING – THE CASE OF Pd AND Au ON DOPED MgO(001)</i>	22
<u>Katarina Batalović</u> , Igor Pašti, Jana Radaković, Carmen Rangel	
<i>MODIFYING THE SURFACE OF NITROGEN-DOPED TiO<sub>2</sub> PHOTOCATALYST WITH PALLADIUM AND PLATINUM</i>	24
<u>Aleksandra Marković</u> , Gunther Wittstock	
<i>SURFACE MODIFICATION BY SELF-ASSEMBLED MONOLAYERS OF FLUORESCENT DYES</i>	25
<u>M. Baljozovic</u> , J. Girovsky, J. Nowakowski, Md. Ehesan Ali, H. R. Rossmann, T. Nijs, E. Aeby, S. Nowakowska, D. Siewert, G. Srivastava, C. Wäckerlin, J. Dreiser, S. Decurtins, Shi-Xia Liu, P. M. Oppeneer, T. A. Jung, N. Ballav	
<i>PHYSICS AND CHEMISTRY ON-SURFACES: INTERFACE MATERIALS CREATED VIA SURFACE ENGINEERING</i>	26
<u>Matic Poberžnik</u> , Anton Kokalj	
<i>ON THE ORIGIN OF SURPRISING ATTRACTIVE INTERACTIONS BETWEEN ELECTRONEGATIVE OXYGEN ADATOMS ON ALUMINUM SURFACES</i>	27
Johan O. Nilsson, Mikael Leetmaa, Baochang Wang, Pjotrs Zguns, Anders Sandell, <u>Natalia V. Skorodumova</u>	
<i>KINETICS OF WATER ADSORPTION ON THE RUTILE TiO<sub>2</sub>(110) SURFACE</i>	29
<b>General session</b>	
<u>Richard G. Compton</u>	
<i>NANO-IMPACTS: NEW INSIGHTS INTO NANOPARTICLES</i>	31
<u>V. Lutsyk</u> , V. Vorob'eva	
<i>4D PHASE DIAGRAMS FOR THE MOLTEN SALT REACTOR MATERIALS</i>	32
<u>Stanislav V. Sokolov</u> , Enno Kätelhön, Richard G. Compton	
<i>NEAR-WALL HINDERED DIFFUSION IN CONVECTIVE SYSTEMS: TRANSPORT LIMITATIONS IN COLLOIDAL AND NANOPARTICULATE SYSTEMS</i>	37

Seyed Ali Nabavi, <u>Goran T. Vladislavljević</u> , Vasilije Manović <i>MANUFACTURING POLYMERIC CAPSULES FOR CO<sub>2</sub> CAPTURE USING MICROFLUIDIC EMULSIFICATION AND ON-THE-FLY PHOTOPOLYMERISATION</i>	38
<b>Hydrogen storage, batteries and electrochemical capacitors</b>	
<u>Anton Gradišek</u> <i>BOROHYDRIDES AS HYDROGEN STORAGE MATERIALS: MOLECULAR DYNAMICS STUDIES</i>	43
<u>I. Milanovic</u> , S. Milosevic, S. Kurko, M. Savic, R. Vujasin, A. Djukic, J. Grbovic Novakovic <i>INFLUENCE OF MILLING TIME ON HYDROGEN DESORPTION PROPERTIES OF LiAlH<sub>4</sub> – Fe<sub>2</sub>O<sub>3</sub> COMPOSITE</i>	44
<u>Sandra Kurko</u> , Radojka Vujasin, Bojana Paskaš Mamula, Jasmina Grbović Novaković, Nikola Novaković <i>DFT STUDY OF HYDROGEN DESORPTION PROPERTIES OF BORON DOPED MgH<sub>2</sub></i>	46
<u>Z. Jovanović</u> , D. Bajuk-Bogdanović, M. Vujković, S. Jovanović, I. Holclajtner-Antunović <i>THE PHYSICOCHEMICAL PROPERTIES OF GRAPHENE OXIDE – PHOSPHOTUNGSTIC ACID HYBRID CAPACITOR</i>	48
<u>Milica Vujković</u> , Slavko Mentus <i>FARADAIC VERSUS PSEUDOCAPACITANCE MECHANISM OF CHARGE STORAGE IN NaFe<sub>0.95</sub>V<sub>0.05</sub>PO<sub>4</sub>/C COMPOSITE</i>	49
<u>Sanja Milošević</u> , Ivana Stojković Simatović, Sandra Kurko, Jasmina Grbović Novaković, Nikola Cvjetičanin <i>VO<sub>2</sub> POLYMORPH B AS A ELECTRODE MATERIAL IN ORGANIC AND AQUEOUS Li-ION BATTERIES</i>	54

## Theory

Milijana Savić, Jana Radaković, Katarina Batalović

*ELECTRONIC STRUCTURE INVESTIGATION OF  $AlH_3$  POLYMORPHS* 59

Sergei I. Simak

*MATERIALS AT HIGH TEMPERATURES: A FIRST-PRINCIPLES THEORY* 60

Jana Radaković, Katarina Batalović, Milijana Savić

*THERMODYNAMICS AND FORMATION MECHANISM OF  $Gd_{0.5}M_{0.5}Cu_5$   
( $M=Mg, Ca$ ) ALLOY FROM FIRST PRINCIPLES* 61

A. V. Ruban

*STRUCTURAL AND ATOMIC CONFIGURATIONAL ASPECTS OF  $Cu_3Pt$   
CATALYSTS* 62

## Electrocatalysis

Milica Vasić, Maria Čebela, Radmila Hercigonja, Diogo M. F. Santos,  
Biljana Šljukić

*Pd-MODIFIED X ZEOLITE ELECTRODES FOR HYDROGEN EVOLUTION  
REACTION IN ALKALINE MEDIUM* 63

Sanjin Gutić, Ana S. Dobrota, Igor A. Pašti

*SIMULTANEOUS ELECTROCHEMICAL REDUCTION OF GRAPHENE OXIDE  
AND DEPOSITION OF NICKEL: EFFECT OF REDUCTION TIME ON  
CATALYTIC PROPERTIES TOWARDS THE HYDROGEN EVOLUTION  
REACTION* 65

Dragana D. Vasić Aničijević, Sladjana Lj. Maslovara, Vladimir M. Nikolić,  
Milica P. Marčeta Kaninski

*IMPROVED HER ACTIVITY OF Ni CATHODE ACTIVATED BY  $NiCoMo$  IONIC  
ACTIVATOR – A DFT ASPECT* 69

<u>Urša Petek</u> , Francisco Ruiz-Zepeda, Martin Šala, Primož Jovanovič, Jonas Pampel, Tim Patrick Fellingner, Vid Simon Šelih, Marjan Bele, Miran Gaberšček <i>THE ROLE OF METAL IMPURITIES IN THE ELECTROCATALYTIC PERFORMANCE OF NITROGEN-DOPED CARBON MATERIAL</i>	73
<u>Nikola Zdolšek</u> , Aleksandra Dimitrijević, Tatjana Trtić-Petrović, Jugoslav Krstić, Danica Bajuk-Bogdanović, Biljana Šljukić <i>FROM GREEN SOLVENT TO CARBON MATERIAL: APPLICATION OF IONIC LIQUID DERIVED CARBON FOR OXYGEN REDUCTION</i>	74
<u>Nemanja Gavrilov</u> , Miloš Stevanović, Igor Pašti, Slavko Mentus <i>INFLUENCE OF NON-AQUEOUS SOLVENTS ON ORR ELECTROCHEMISTRY</i>	75
<u>Viktor Čolić</u> , Aliaksandr Bandarenka <i>Pt-ALLOY ELECTROCATALYSTS FOR THE OXYGEN REDUCTION REACTION: FROM MODEL SURFACES TO NANOSTRUCTURED SYSTEMS</i>	76
<b>Electrocatalyst stability/DURAPEM session</b>	
A. Pavlišić, P. Jovanovič, V. S. Šelih, M. Šala, M. Bele, G. Dražić, I. Arčon, S. Hočevar, A. Kokalj, N. Hodnik, <u>M. Gaberšček</u> <i>HOW TO IMPROVE THE STABILITY OF PLATINUM-BASED ELECTROCATALYSTS?</i>	77
<u>Nejc Hodnik</u> , Primož Jovanovič, Matija Gatalo, Francisco Ruiz-Zepeda, Marjan Bele, Miran Gaberšček <i>ADVANCED CHARACTERIZATION ELECTROCHEMICAL METHODS FOR STUDYING NANOPARTICLE ELECTROCATALYSTS STABILITY</i>	78
<u>Primož Jovanovič</u> , Andraž Pavlišić, Vid Simon Šelih, Martin Šala, Samo Hočevar, Marjan Bele, Francisco Ruiz-Zepeda, Goran Dražić, Nejc Hodnik, Miran Gaberšček <i>ELECTROCATALYSTS STABILITY INVESTIGATION BY ELECTROCHEMICAL FLOW CELL ANALYTICS</i>	79

---

<u>Matija Gatalo</u> , Primož Jovanovič, Jan-Philipp Grote, Francisco Ruiz-Zepeda, Nejc Hodnik, Goran Dražič, Marjan Bele, Karl J.J. Mayrhofer, Miran Gaberšček	
<i>TUNING THE STABILITY OF PtCu<sub>3</sub>/C ORR ELECTROCATALYST WITH GOLD DECORATION AND GOLD DOPING</i>	80
<hr/>	
<u>Ana S. Dobrota</u> , Igor A. Pašti	
<i>FIRST PRINCIPLES INSIGHTS INTO GRAPHENE ELECTRONIC AND CHEMICAL PROPERTIES MODIFICATION BY SUBSTITUTIONAL DOPING</i>	81
<hr/>	
<u>Ivan Stoševski</u> , Jelena Krstić, Zorica Kačarević-Popović, Šćepan Miljanić	
<i>INVESTIGATION OF THE RADIOLITICALLY SYNTHESIZED Ag/C CATALYST AS A POTENTIAL CATHODE MATERIAL OF AN ALKALINE FUEL CELL USING NEWLY DESIGNED GAS-FLOW HALF-CELL</i>	82

---





***Plenary lectures***

---



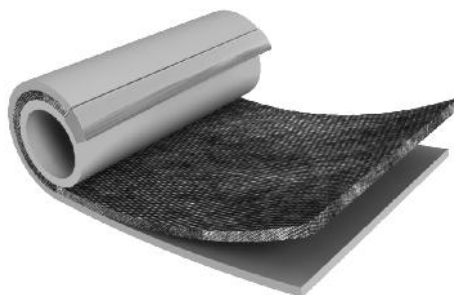
# LANTHANOIDE DOPED $\delta$ -Bi<sub>2</sub>O<sub>3</sub> WITH ENHANCED CONDUCTIVITY

Aleksandra Dapčević

*Faculty of Technology and Metallurgy, University of Belgrade, Karnegijeva 4,  
Belgrade, Serbia*

Due to the increasing need for new highly efficient and environmentally friendly energy conversion technologies, the oxide ion conductors applicable in solid oxide fuel cells (SOFCs) have widely been investigated. The aim is to find an electrolyte with enhanced stability over a wide temperature range with the ionic conductivity high enough at intermediate temperatures in order to reduce the operating temperature of SOFCs. The high temperature  $\delta$ -Bi<sub>2</sub>O<sub>3</sub> phase has been proposed as a good candidate for electrolyte in SOFCs because it is the fastest known ionic conductor.

One method of the stabilization of O<sup>2-</sup> ion conductors related to the  $\delta$ -Bi<sub>2</sub>O<sub>3</sub> polymorph in Bi<sub>2</sub>O<sub>3</sub>-Tm<sub>2</sub>O<sub>3</sub> and Bi<sub>2</sub>O<sub>3</sub>-Lu<sub>2</sub>O<sub>3</sub> systems by using the solid state reaction is shown in this study. Six starting mixtures with the following compositions (Bi<sub>1-x</sub>Tm<sub>x</sub>)<sub>2</sub>O<sub>3</sub>,  $x = 0.11$ , 0.14 and 0.20, and (Bi<sub>1-y</sub>Lu<sub>y</sub>)<sub>2</sub>O<sub>3</sub>,  $y = 0.15$ , 0.20 and 0.25, were dry



homogenized in an agate mortar, heat treated at 750 °C for 3 h and then slowly furnace cooled. The samples were characterized by XRD, TEM/SAED, SEM, DTA and EIS techniques. The effect of thermal aging was investigated as well by heating the obtained samples firstly at 700 °C, then cooling down to 500 °C for three days and finally reheating at 700 °C.

Based on XRD and TEM/SAED, the targeted cubic lanthanoid doped  $\delta$ -Bi<sub>2</sub>O<sub>3</sub> single-phase samples (space group  $Fm\bar{3}m$ ) were successfully obtained within all six systems. The unit cell parameter of both Tm- and Lu-doped  $\delta$ -Bi<sub>2</sub>O<sub>3</sub> decreases as dopant content increases. By comparing Tm- and Lu-doped  $\delta$ -Bi<sub>2</sub>O<sub>3</sub> phases mutually, an expected increase of the unit cell with larger ionic radii of dopant was found [ $r_i(\text{Tm}^{3+}) = 0.88 \text{ \AA}$ , and  $r_i(\text{Lu}^{3+}) = 0.86 \text{ \AA}$  in the octahedral environment<sup>1</sup>].

Electrochemical impedance of  $\delta$ -Bi<sub>2</sub>O<sub>3</sub> phases was measured between 300 and 800 °C. At temperatures 550 – 800 °C the conductivities are of the same order of magnitude (0.1 – 0.4 S cm<sup>-1</sup>), but with lowering temperature they rapidly decrease resulting in two activation energies. This is due to the changes in change in charge carrier mobility. The EIS also did not show any evidence of the grain boundary contribution to the conductivity being in accordance with SEM analysis, which revealed relatively large grains that were 10 – 25  $\mu\text{m}$  in

diameter. The porosity in the form of closed pores is barely present. This is important since the electrolyte applicable in SOFC should be dense and non-porous.

According to the cyclic DTA curves, no phase transitions were observed in the following samples:  $(\text{Bi}_{0.8}\text{Tm}_{0.2})_2\text{O}_3$ ,  $(\text{Bi}_{0.8}\text{Lu}_{0.2})_2\text{O}_3$  and  $(\text{Bi}_{0.75}\text{Lu}_{0.25})_2\text{O}_3$ , indicating that these doped  $\delta\text{-Bi}_2\text{O}_3$  phases are thermally stable within the whole investigated interval, *i.e.* from room temperature to 985 °C. Moreover, no evidence of structural aging was found for these samples.

Such stability and extraordinary conductivities allow the application of these electrolyte materials in IT-SOFC resulting not only in the significant enhancement of fuel cell's electrochemical performance, but also in its good structural stability over long time service in a wide temperature range. Moreover, these promising electrolytes do not undergo any changes in dimension and thus can provide durable and crack-free fuel cell stacks.

#### References

[1] R. D. Shannon, *Acta Cryst.* 1976, **A 32**, 751.

# HYDROGEN OXIDATION: FROM THERMODYNAMICS TO THE REACTION KINETICS AT SINGLE NANOPARTICLES

Chris Batchelor-McAuley

*Department of Chemistry, Physical and Theoretical Chemistry Laboratory, Oxford University, South Parks Road, Oxford OX1 3QZ, U.K.*

Although a paradigmatic and highly studied reaction the proton/hydrogen redox couple is still of distinct physical and theoretical interest. This talk will start by aiming to clearly demonstrate and clarify the voltammetric response of this 'inner-sphere' redox couple under reversible electrochemical conditions. Due to the process involving an ion-transfer across the double layer, the plausible importance and influence of the double layer will also be considered briefly.

Experimentally, as the size of the electrode is decreased from macro- to micro-scopic dimensions the oxidative current becomes limited by the rate of hydrogen adsorption to the interface. The talk will proceed by providing examples of the hydrogen oxidation reaction at the micro and nanoscales. Experimentally it will be demonstrated how the voltammetric reaction can be studied both at single palladium coated carbon nanotubes and individual platinum nanoparticles.

## References

- [1] X. Jiao, C. Batchelor-McAuley, E. Kätelhön, J. Ellison, K. Tschulik, R.G. Compton J. Phys. Chem. C, 2015, **119**, 9402-9410.
- [2] C. Lin, E. Laborda, C. Batchelor-McAuley, R.G. Compton, Phys. Chem. Chem. Phys., 2016, **18**, 9829-9837.
- [3] X. Li, C. Batchelor-McAuley, S.A.I. Whitby, K. Tschulik, L. Shao, R.G. Compton, Angew. Chem., 2016, **128**, 4368 –4371.
- [4] X. Jiao, C. Lin, N.P. Young, C. Batchelor-McAuley, R.G. Compton, J. Phys. Chem. C, 2016, **120**, 13148–13158.



***Solid electrolytes and oxide materials  
for energy related applications***

---





# CRYSTALLIZATION PATHS IN CERAMIC SYSTEMS WITH THE MATERIALS FOR ENERGY APPLICATION

V. Lutsyk<sup>1,2\*</sup>, A. Zelenaya<sup>1</sup>, M. Parfenova<sup>3</sup>

<sup>1</sup>*Institute of Physical Materials Science, 6 Sahyanova st., 670047 Ulan-Ude, Russia (\*vluts@ipms.bscnet.ru);* <sup>2</sup>*Buryat State University, 24a Smolin st., 670000 Ulan-Ude, Russia;* <sup>3</sup>*Tomsk State University of Control Systems and Radio-electronics, 634050 Tomsk, Russia*

Investigation of silicate systems  $\text{Li}_2\text{O}-\text{FeO}-\text{SiO}_2$ ,  $\text{Li}_2\text{O}-\text{MnO}-\text{SiO}_2$  is promising for compounds  $\text{Li}_2\text{FeSiO}_4$ ,  $\text{Li}_2\text{MnSiO}_4$  preparation, which are used as electrode materials [1-2]. Other oxide materials, as  $\text{Ce}_{1-x}\text{Bi}_x\text{O}_{2-\delta}$  ( $x=0.1-0.5$ ) solid solution are perspective at application in solid oxide fuel cell (SOFC) [3], and  $\text{NiFe}_2\text{O}_4$  can be used for the cathode production [4]. Elaboration of computer models of phase diagrams (PD) for oxide systems permit to expand the possibilities of their investigation. The dividing on two, one and zero-dimensional concentration fields (obtained by projecting all PD elements into Gibbs triangle) are made, all possible crystallization schemes and the content of each microstructural component with regard to its origin are considered on a basis of PD models [5]. The particularities of processes for different concentration fields can be examined by the diagrams of vertical mass balance, which show the increase or decrease of phase portion for each phase region. Also they allow to compare qualitatively the concentration field with different schemes of phase reactions, but with the same microconstituents. Forecast of microconstituents for concentration fields of different dimensions permit to reduce and plan further experimental study. Systems  $\text{TiO}_2-\text{SiO}_2-\text{Al}_2\text{O}_3$ ,  $\text{TiO}_2-\text{ZrO}_2-\text{Al}_2\text{O}_3$ ,  $\text{TiO}_2-\text{ZrO}_2-\text{SiO}_2$ ,  $\text{ZrO}_2-\text{SiO}_2-\text{Al}_2\text{O}_3$ ,  $\text{CaO}-\text{SiO}_2-\text{Al}_2\text{O}_3$  and  $\text{MgO}-\text{SiO}_2-\text{Al}_2\text{O}_3$  [5-6] can be used to demonstrate the potential of their space computer models [5-6].

## Acknowledgement

This work has been performed under the program of fundamental research SB RAS (project 0336-2014-0003) and was partially supported by the Russian Foundation for Basic Research (projects 14-08-00453, 15-43-04304).

## References

- [1] DL. Yan, XF. Geng, YM. Zhao, XH. Lin, XD. Liu, J. Mater. Sci., 2016, **51**, 6452–6463.
- [2] A. Kokalj, R. Dominko, G. Mali, A. Meden, M. Gaberšček, J. Jamnik, Abs. 1<sup>st</sup> Workshop on Mater. Sci. for Energy Related Applic., Belgrade (Serbia), 2014, 10.
- [3] M. Prekajski, B. Matović M. Stojmenović, G. Branković, Ibid, 16-17.
- [4] D. Chanda, J. Hnát, M. Paidar, K. Bouzek, Ibid, 22-24.

- [5] V. Lutsyk, A. Zelenaya, A. Zyryanov, E. Nasrulin, *Építőanyag – J. Silicate Based and Composite Materials*, 2016, **68**, 52-55.
- [6] V.I. Lutsyk, V.P. Vorob'eva, A.E. Zelenaya, *Solid State Phenomena*, 2015, **230**, 51-54.

# CHEMICAL STABILITY OF DOPED $\text{BaCe}_{0.9}\text{Y}_{0.1}\text{O}_{3-\delta}$ AS A PROTON CONDUCTING ELECTROLYTE FOR IT-SOFC

A. Radojković, M. Žunić, S. Savić, Z. Branković, G. Branković

*Institute for Multidisciplinary Research, University of Belgrade,  
Kneza Višeslava 1a, 11030 Belgrade, Serbia*

$\text{BaCe}_{0.9}\text{Y}_{0.1}\text{O}_{3-\delta}$  (BCY) has been one of the most studied materials known for its highest proton conductivity at temperatures between 500 and 700 °C, which allows its application as a proton conducting electrolyte for intermediate-temperature solid oxide fuel cells (IT-SOFC). The proton conductivity is an exclusive property of mixed oxides with perovskite structure and large unit cell volume, such as  $\text{BaCeO}_3$  or  $\text{SrCeO}_3$ . Doping with aliovalent cations ( $\text{Y}^{3+}$ ) that replace  $\text{Ce}^{4+}$  induces formation of point defects (oxygen vacancies), which in wet or hydrogen containing atmosphere allow proton mobility. The main disadvantage of this material is its instability in  $\text{CO}_2$ -rich atmosphere due to the basic character of the crystal lattice, thus limiting its application in SOFCs in respect to fuel selection. However, the stability of BCY can be enhanced by doping with cations that may raise the acidic character of the material, such as  $\text{Nb}^{5+}$ ,  $\text{Ta}^{5+}$  or  $\text{In}^{3+}$ . Introduction of pentavalent cations will lead to reduced amount of point defects and consequently lower proton conductivity and it is therefore recommended that their molar concentration should not exceed 5 %. On the other hand, trivalent  $\text{In}^{3+}$  is more suitable as it can completely replace  $\text{Y}^{3+}$  since it can both serve as a point defect source and increase acidity of the crystal lattice. Because of these properties it can be introduced in much larger amounts than  $\text{Nb}^{5+}$  or  $\text{Ta}^{5+}$ .

In this study  $\text{BaCe}_{0.9-x}\text{Nb}_x\text{Y}_{0.1}\text{O}_{3-\delta}$  (where  $x = 0.01, 0.03$  and  $0.05$ ) and  $\text{BaCe}_{1-x}\text{In}_x\text{O}_{3-\delta}$  (where  $x = 0.15, 0.20$  and  $0.25$ ) powders were synthesized by the method of autocombustion, while  $\text{BaCe}_{0.9-x}\text{Ta}_x\text{Y}_{0.1}\text{O}_{3-\delta}$  (where  $x = 0.01, 0.03$  and  $0.05$ ) powders were prepared by the classical solid state route. Much higher specific surface areas were observed for the samples synthesized by the autocombustion method. In the case of Nb and Ta doped samples, the dense electrolytes were formed after sintering at 1550 °C for 5 h in air. Temperature of 1300 °C was enough to complete sintering of the samples doped with In after 5 h in air, which was another advantage of In as a dopant. The conductivities determined by impedance measurements in temperature range of 550-700 °C in wet hydrogen showed a decreasing trend with increase of Nb and Ta content, while it was the opposite in the case of In. Interestingly, the total conductivity of the samples  $\text{BaCe}_{0.85}\text{Nb}_{0.05}\text{Y}_{0.1}\text{O}_{3-\delta}$ ,  $\text{BaCe}_{0.85}\text{Ta}_{0.05}\text{Y}_{0.1}\text{O}_{3-\delta}$  and  $\text{BaCe}_{0.75}\text{In}_{0.25}\text{O}_{3-\delta}$  reached around  $5 \times 10^{-3}$  S/cm in wet hydrogen atmosphere at 700 °C. After exposure in 100 %  $\text{CO}_2$  atmosphere at 700 °C for 5 h, the samples were

investigated by X-ray analysis. It was found that even 15 % In could completely suppress degradation of electrolyte, while the highest concentrations of Nb and Ta (5%) were necessary to secure sufficient stability in CO<sub>2</sub>.

# IONIC CONDUCTIVITY IN DOPED CERIA FROM AB INITIO NON-EQUILIBRIUM MOLECULAR DYNAMICS COMBINED WITH A COLOR- DIFFUSION ALGORITHM

Olga Yu. Vekilova<sup>1,2</sup>, Johan O. Nilsson<sup>1</sup>, Johan Klarbring<sup>3</sup>, Sergei I. Simak<sup>3</sup>,  
Natalia V. Skorodumova<sup>1,2</sup>

<sup>1</sup>*Materials Science and Engineering, KTH - Royal Institute of Technology,  
Brinellvägen 23, 100 44 Stockholm, Sweden;* <sup>2</sup>*Department of Physics and  
Astronomy, Uppsala University, Box 516, 751 20 Uppsala, Sweden;*

<sup>3</sup>*Department of Physics, Chemistry and Biology (IFM), Linköping University, SE-  
581 83 Linköping, Sweden*

The energy related materials are the hot topic of modern research in materials science and engineering. Sources of “green” energy provide the society with energy without polluting the environment. The solid oxide fuel cells (SOFCs) are an attractive “green” alternative to fossil fuels. Understanding of the diffusion properties of electrolytic systems is of high practical importance for the modern development of SOFC. For this aim the non-equilibrium molecular dynamics is a powerful technique giving a possibility to theoretically study the diffusion in systems at high temperatures. Coupled with the color-diffusion algorithm it substantially decreases simulation time; allowing one to study diffusion from first principles [1]. This approach has been successfully applied to study the oxygen diffusion coefficient and bulk ionic conductivity in doped ceria at temperatures around 1000 K [2-3]. Good agreement with the existing experiment data is obtained.

## References

- [1] P.C. Aeberhard, S.R. Williams, D.J. Evans, K. Refson, W.I.F. David, Phys. Rev. Lett., 2012, **108**, 095901.
- [2] J.O. Nilsson, O.Yu. Vekilova, O. Hellman, J. Klarbring, S.I. Simak, N.V. Skorodumova, Phys. Rev. B, 2016, **93**, 024102.
- [3] J. Klarbring, O.Yu. Vekilova, J.O. Nilsson, N.V. Skorodumova, S.I. Simak, accepted to Solid State Ionics, 2016.

# **SIMULATION OF ION CONDUCTIVITY IN DOPED CERIA FROM FIRST PRINCIPLES**

Johan O. Nilsson<sup>1</sup>, Mikael Leetmaa<sup>2</sup>, Olga Yu. Vekilova<sup>2</sup>, Sergei I. Simak<sup>3</sup>,  
Natalia V. Skorodumova<sup>1,2</sup>

*<sup>1</sup>Department of Materials Science and Engineering, KTH - Royal Institute of  
Technology, Brinellvägen 23, 100 44 Stockholm, Sweden; <sup>2</sup>Department of Physics  
and Astronomy, Uppsala University, Box 516, 751 20 Uppsala, Sweden;*

*<sup>3</sup>Department of Physics, Chemistry and Biology (IFM), Linköping University, 581  
83, Linköping, Sweden*

We examine the effect of dopant type and dopant distribution on the ion diffusion in ceria doped with rare-earth elements. Diffusion is simulated by means of Kinetic Monte Carlo using transition rates derived from the diffusion barriers calculated in the framework of density functional theory. Based on the diffusion simulations, we discuss the characteristics of a good dopant in terms of diffusion barriers and study oxygen ion trajectories for different dopants and distributions. For many first-principles methods, simulations of diffusion in solids produce poor statistics of diffusion events. We present an analytical expression for the statistical error in ion conductivity obtained in such simulations. The error expression is not restricted to any computational method in particular, but valid in the context of simulation of Poisson processes in general. This analytical error expression is verified numerically for the case of Gd-doped ceria by running a large number of Kinetic Monte Carlo calculations.

## THERMOELECTRIC PROPERTIES OF $\text{NaCo}_{2-x}\text{Cu}_x\text{O}_4$ ( $x = 0, 0.01, 0.03, 0.05$ ) CERAMIC

Sanja Pršić<sup>1</sup>, Slavica M. Savić<sup>1,2</sup>, Zorica Branković<sup>1</sup>, Stanislav Vrtnik<sup>3</sup>,  
Slavko Bernik<sup>4,5</sup>, Goran Branković<sup>1</sup>

<sup>1</sup>*Institute for Multidisciplinary Research, University of Belgrade, Kneza Višeslava 1, 11030 Belgrade, Serbia;* <sup>2</sup>*Biosense Institute-Institute for Research and Development of Information Technology in Biosystems, Dr Zorana Đinđića 1, 21000 Novi Sad, Serbia;* <sup>3</sup>*Jožef Stefan Institute, Condensed Matter Physics, Jamova cesta 39, 1000 Ljubljana, Slovenia;* <sup>4</sup>*Jožef Stefan Institute, Department for Nanostructured Materials, Jamova cesta 39, 1000 Ljubljana, Slovenia;* <sup>5</sup>*Center of Excellence NAMASTE, Jamova cesta 39, 1000 Ljubljana, Slovenia*

Layered cobalt oxides have attracted great attention during past decade as potential candidates for thermoelectric application. However, the scientists are dealing with several problems concerning synthesis, Na evaporation, changes of the stoichiometry of the ceramic, etc. In order to reduce synthesis duration and temperature, prevent Na evaporation and improve mixing of the precursors we applied mechanochemically assisted solid state reaction and citric acid complex methods to obtain  $\text{NaCo}_{2-x}\text{Cu}_x\text{O}_4$  ( $x = 0, 0.01, 0.03, 0.05$ ) powders. Ceramic samples were prepared by pressing into disc-shaped pellets and subsequently sintered at 880 °C in inert argon atmosphere. The electrical resistivity ( $\rho$ ), the thermal conductivity ( $\kappa$ ) and the Seebeck coefficient ( $S$ ) were measured simultaneously in the temperature range from 2 K to 830 K, and the effect of small concentrations of the dopant on the thermoelectric properties was observed. It was found that in the low temperature range  $\rho$  increased with temperature, indicating metallic behavior. The values of  $\kappa$  decreased as the temperature increased.  $S$  was higher in all Cu-doped samples, reaching 145  $\mu\text{V/K}$  at 830 K for  $x = 0.03$ , and this suggested strong electron correlation in these systems. The highest figure of merit ( $ZT$ ) at room temperature (0.022) was obtained for  $x = 0.01$  prepared by the citric acid complex method and it was twice higher than in undoped sample. In the temperature region between 300 K and 830 K, higher  $ZT$  was also obtained for the samples prepared by citric acid complex method, reaching the value of 0.056 at 830 K for  $x = 0.05$  and it was almost three times higher than in undoped sample. These results confirm that even small concentration of Cu significantly influences the thermoelectric properties of  $\text{NaCo}_2\text{O}_4$ .





***Heterogeneous catalysis  
and  
Photocatalysis***

---



# SYNTHESIS OF METAL GLYCEROLATES AS CATALYSTS FOR BIODIESEL PRODUCTION

Ivana Lukić<sup>1</sup>, Željka Kesić<sup>1</sup>, Miodrag Zdujić<sup>2</sup>, Dejan Skala<sup>1</sup>

<sup>1</sup>*University of Belgrade, Faculty of Technology and Metallurgy, Belgrade, Serbia;*

<sup>2</sup>*Institute of Technical Sciences of the Serbian Academy of Sciences and Arts, Belgrade, Serbia*

Mechanochemical treatment of metal oxides (CaO, ZnO) and mixed metal oxides (CaO·ZnO, mixture of CaO and ZnO) suspended in glycerol was performed in order to prepare metal glycerolates. Obtained material was characterized by infrared spectroscopy (FTIR), X-ray diffraction (XRD), thermal analysis (TGA/DTA), and Hammett indicator method for base strength determination.

Results revealed that Ca glycerolate (CaG) was successfully synthesized by mechanochemical treatment of CaO and glycerol, while in the case of ZnO it was not possible to completely obtain corresponding glycerolate (ZnG) even under diverse conditions of mechanochemical treatment (molar ratio of metal oxide and glycerol, duration of treatment, angular velocity of disc and addition of alkali). On the contrary, by heating ZnO and glycerol at 160 °C for 1 h, characterization proved that single-phase ZnG was obtained. CaO·ZnO was partly converted into glycerolate (CaZnG) by mechanochemical treatment.

Prepared CaG showed a high catalytic activity in methanolysis of sunflower oil under different reaction conditions, while with CaZnG only moderate yield (around 60%) of fatty acid methyl esters (FAME) was achieved at 60 °C after 6h.

## Acknowledgement

Financial support of the Ministry of Education and Science of the Republic of Serbia (Grant No. 45001) is gratefully acknowledged.

## PHOTOCATALYTIC PROPERTIES OF $\text{BiFeO}_3$ PARTICLES SYNTHESIZED BY ULTRASOUND SOL-GEL ASSISTED ROUTE

Iovana Ćirković, Danijela Luković Golić, Aleksandar Radojković, Aleksandra Dapčević, Zorica Branković, Goran Branković

*Institute for multidisciplinary research, University of Belgrade, Kneza Višeslava 1, Serbia*

$\text{BiFeO}_3$  precursor powder was synthesized by ultrasound assisted sol-gel route at relatively low temperature, starting from Bi-nitrate, Fe-nitrate, and ethylene glycol. Structural, optical, and photocatalytic properties of obtained powder were investigated. X-ray diffraction analysis confirmed that thermal treatment of precursor powder at 500 °C, led to formation of pure phase  $\text{BiFeO}_3$ . The determined band gap was 2.20 eV, indicating its potential application as visible-light-response photocatalyst. The photocatalytic behaviour of  $\text{BiFeO}_3$  powder was estimated by the degradation of Reactive Orange 16 (RO16), typical azo dye. Photocatalytic activities under different pH values were further studied. The result shows that the  $\text{BiFeO}_3$  particles exhibit the highest photocatalytic activity in the solution with the lowest pH value.

# **SURFACE MODIFICATION OF ANATASE NANOPARTICLES MODIFIED WITH CATECHOLATE TYPE LIGANDS: EXPERIMENTAL AND DFT STUDY OF OPTICAL PROPERTIES**

T. D. Savić<sup>1\*</sup>, M. I. Čomor<sup>1</sup>, I. A. Janković<sup>1</sup>, D. Ž. Veljković<sup>2</sup>, S. D. Zarić<sup>2</sup>

<sup>1</sup>*Vinča Institute of Nuclear Sciences, University of Belgrade, P.O. Box 522, 11001 Belgrade, Serbia (\*[tanja030@vinca.rs](mailto:tanja030@vinca.rs));* <sup>2</sup>*Department of Chemistry, University of Belgrade, Studentski trg 16, P.O.Box 158, 11001 Belgrade, Serbia*

The surface modification of nanocrystalline TiO<sub>2</sub> particles (45 Å) with catecholate-type ligands consisting of an extended aromatic ring system (2,3-dihydroxynaphthalene and anthrarobin) [1] and different electron donating/electron withdrawing substituent groups (3-methylcatechol, 4-methylcatechol, 3-methoxycatechol, 3,4-dihydroxybenzaldehyde and 4-nitrocatechol)[2] was found to alter the optical properties of nanoparticles in a similar way to catechol. The formation of the inner-sphere charge transfer (CT) complexes results in a red shift of the semiconductor absorption compared to unmodified nanocrystallites and a reduction of the effective band gap upon the increase of the electron delocalization on the inclusion of additional rings. Additionally, these effects are slightly less pronounced in the case of electron withdrawing substituents. The investigated ligands have the optimal geometry for binding to surface Ti atoms, resulting in ring coordination complexes of the catecholate type (binuclear bidentate binding-bridging) thus restoring six-coordinated octahedral geometry of surface Ti atoms. From the absorption measurements (Benesi-Hildebrand plot), the stability constants in methanol/water = 90/10 solutions at pH 2 in the order of 10<sup>3</sup> M<sup>-1</sup> have been determined. The binding structures were investigated by using FTIR spectroscopy. Quantum chemical calculations on model systems using density functional theory (DFT, B3LYP level of theory) were performed to obtain the HOMO-LUMO gaps and vibrational frequencies of CT complexes. The calculated values were compared with the experimental data proving the more probable binding structures.

## References

- [1] T. D. Savić, I. A. Janković, Z. V. Šaponjić, M. I. Čomor, D. Ž. Veljković, S. D. Zarić, J. M. Nedeljković, *Nanoscale*, 2012, **4**, 1612 – 1619.
- [2] T. D. Savić, M. I. Čomor, J. M. Nedeljković, D. Ž. Veljković, S. D. Zarić, V. M. Rakić, I. A. Janković, *Phys. Chem. Chem. Phys.* 2014, **16** (38), 20796-20805.

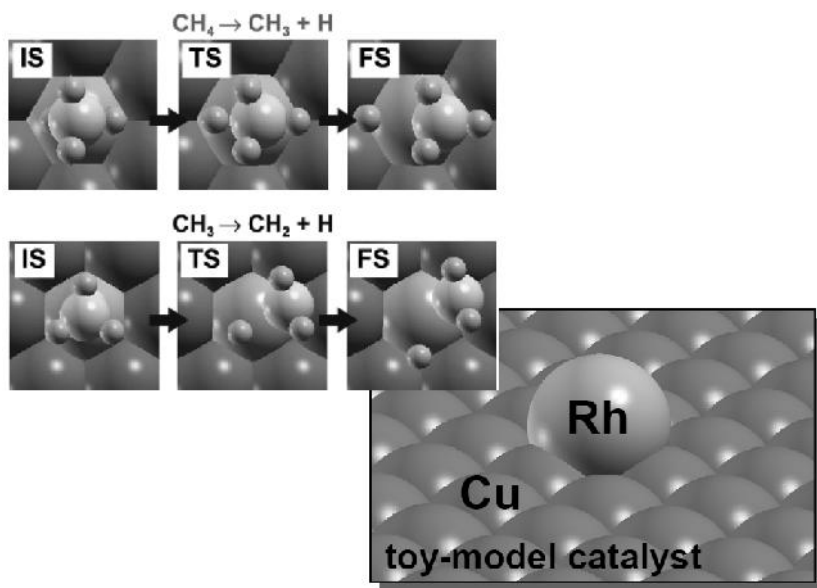
# A MODEL STUDY OF METHANE DEHYDROGENATION ON Rh@Cu(111)

Anton Kokalj

*Department of Physical and Organic Chemistry, Jožef Stefan Institute, SI-1000  
Ljubljana, Slovenia ([tone.kokalj@ijs.si](mailto:tone.kokalj@ijs.si))*

Tuning the relative reaction rates of the different steps of methane dehydrogenation would allow for the optimal design of many dream reactions such as, e.g., the direct conversions of methane to methanol, to formaldehyde, or to higher hydrocarbons. The efficiency of transition-metal catalysts to promote these and other related reactions is limited by the tendency of dehydrogenation to proceed until graphite is eventually formed on the surface, thus poisoning the catalyst.

The issue of tuning the relative height of the first two dehydrogenation barriers of methane ( $\text{CH}_4 \rightarrow \text{CH}_3 + \text{H}$  and  $\text{CH}_3 \rightarrow \text{CH}_2 + \text{H}$ ) was addressed using density-functional theory. A careful analysis of the results of computer simulations allows one to disentangle the mechanisms which determine the reactivity of a specific (model) catalyst at the nanometric scale. In the particular case, based on such an analysis, we shown that the combination of a very active reaction center—such as Rh—with a more inert substrate—such as Cu(111)—may hinder the second dehydrogenation step with respect to the first, thus resulting in the reverse of the natural order of the two barriers' heights [1].



This work has been done in collaboration with N. Bonini, S. de Gironcoli, C. Sbraccia, G. Fratesi, and S. Baroni from SISSA/DEMOCRITOS, Trieste, Italy.

#### References

[1] A. Kokalj, N. Bonini, S. de Gironcoli, C. Sbraccia, G. Fratesi, S. Baroni, J. Am. Chem. Soc. 2006, **128**, 12448–12454.

## VISIBLE-LIGHT RESPONSIVE Al<sub>2</sub>O<sub>3</sub> PARTICLES

Vesna Đorđević<sup>1</sup>, Jasmina Dostanić<sup>2</sup>, Davor Lončarević<sup>2</sup>, S. Phillip Ahrenkiel<sup>3</sup>,  
Dušan N. Sredojević<sup>4</sup>, Nenad Švrakić<sup>4,5</sup>, Jovan M. Nedeljković<sup>1</sup>

<sup>1</sup>*Institute of Nuclear Sciences Vinča, University of Belgrade, P.O. Box 522, 11001 Belgrade, Serbia;* <sup>2</sup>*Institute of Chemistry, Technology and Metallurgy, University of Belgrade, Studentski trg 12-16, 11000 Belgrade, Serbia;* <sup>3</sup>*South Dakota School of Mines and Technology, 501 E. Saint Joseph Street, Rapid City, SD 57701, USA;*

<sup>4</sup>*Texas A&M University at Qatar, P.O. Box 23874, Doha, Qatar;* <sup>5</sup>*Institute of Physics, University of Belgrade, Pregrevica 118, 11080 Belgrade, Serbia*

The introduction of band structure engineering techniques in the design of hybrid photo-sensitive devices has opened the possibility to manufacture a wide range of novel solar-light responsive materials by manipulating their band gaps and band edges. Here we present a detailed study of Al<sub>2</sub>O<sub>3</sub> - an insulator with the band gap of about 8.7 eV in its nascent state - and investigate the range of its different organic/inorganic charge transfer (CT) complexes for visible-light photo activity. Our results show that coordination of small colorless organic molecules with the surface of Al<sub>2</sub>O<sub>3</sub> particles lead to the formation of composites whose optical absorption is extended in the visible spectral region. The optical property and photocatalytic ability of surface-modified Al<sub>2</sub>O<sub>3</sub> particles were discussed in terms of relative position of energy levels. The quantum chemical calculations were performed using density functional theory (DFT), and the values of calculated HOMO–LUMO gaps for a series of aluminum complex model systems were compared with the experimentally determined band gap values. Also, photocatalytic reactions, driven using surface-modified Al<sub>2</sub>O<sub>3</sub> particles indicate that the CT complex formation is a promising way to enhance photocatalytic performance of metal oxides.



## NANOSIZED ANATASE PARTICLES FOR APPLICATION IN DYE-SENSITIZED SOLAR CELLS (DSSCs)

Nikola Tasić<sup>1</sup>, Zorica Marinković Stanojević<sup>1</sup>, Zorica Branković<sup>1</sup>,  
Uroš Lačnjevac<sup>1</sup>, Milan Žunić<sup>2</sup>, Martina Gilić<sup>3</sup>, Goran Branković<sup>1</sup>

*<sup>1</sup>Department of Materials Science, Institute for Multidisciplinary Research, University of Belgrade, Serbia; <sup>2</sup>Department of Basic Sciences, College of Engineering and Information Technology, University of Business and Technology, Jeddah, Saudi Arabia; <sup>3</sup>Institute of Physics, University of Belgrade, Serbia*

Dye-sensitized solar cells (DSSCs) are 3<sup>rd</sup> generation photovoltaic devices, which convert solar to electric power by utilization of photosensitive dye molecules anchored on the surface of highly porous titania (TiO<sub>2</sub>) thick film. In this work, we have compared the photovoltaic performance of DSSCs in which we have used titania films prepared from either commercially available nano-TiO<sub>2</sub> powder or hydrothermally-assisted sol-gel synthesized nanoanatase. Morphology and dimensions of synthesized nanoparticles were investigated using transmission electron microscopy (TEM) and field-emission scanning electron microscopy (FE-SEM). The presence of anatase crystallographic phase was confirmed by X-ray diffraction (XRD) pattern, selected-area electron diffraction (SAED) pattern, and Raman spectra. Desirable high transparency of the films in the visible region was observed in the optical UV-VIS-NIR spectra. The mesoporosity and uniformity of the films obtained from both powders were confirmed by the scanning electron microscopy (SEM).

DSSCs were fabricated using as prepared films and commercially available Ru- dye (N719) and iodine-based electrolyte. For the photovoltaic measurements, as fabricated cells were illuminated with 300W halogen light source at 1000 W·m<sup>-2</sup> and their current density-voltage (J-V) characteristics were registered. The charge transport phenomena in cells were investigated using electrochemical impedance spectroscopy (EIS), and by recording open-circuit voltage decay curves (OCVD). The cells with synthesized TiO<sub>2</sub> exhibited excellent short-current density ( $J_{sc}$ ) response, up to 11.7 mA cm<sup>-2</sup>, with the average photo-to-current efficiency of 5.0%, while the best photovoltaic response of cells with purchased titania particles was 4.3% ( $J_{sc}$ =9.5 mA cm<sup>-2</sup>).

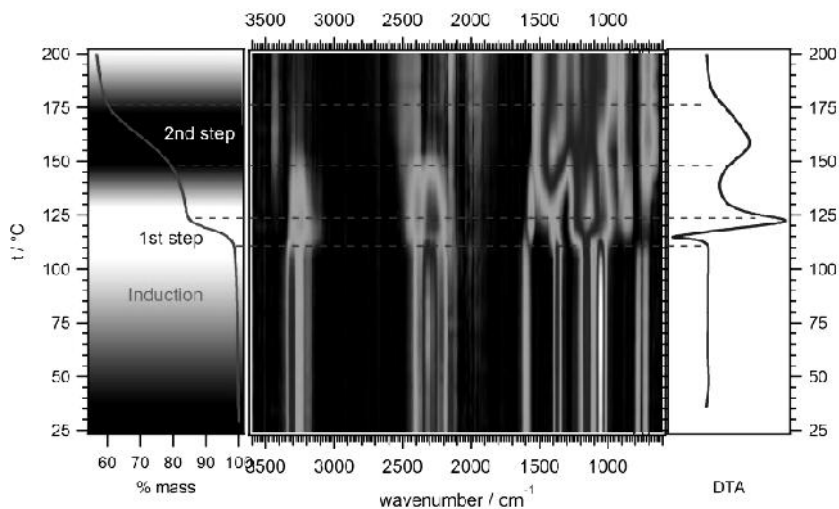
# IN-SITU TEMPERATURE DEPENDENT INFRARED SPECTROSCOPY OF AMMONIA BORANE DEHYDROGENATION

Nikola Biliškoy, Danijela Vojta

*Rudjer Boskovic Institute, Bijenička c. 54, Zagreb, Croatia*

Infrared spectroscopy (IR) is one of the commonly employed experimental methods for the study of hydrogen sorption performance of complex hydrides, but its full power is not well recognised among researchers. It is used almost exclusively as supporting routine. However, IR spectra give a unique insight into the system at molecular level and they are very rich in contained information. For example, detection of phase changes is enabled by simple and straightforward analysis of perturbation-dependent (where perturbation can be temperature, pressure etc.) transmission baseline, while molecular background of these transitions are obtained by the analysis of other spectral features. Furthermore a combination of ATR and transmission technique enables a resolution of the processes in the bulk from those occurring at near-surface level. Also, IR spectroscopy is well recognized as one of the most powerful experimental techniques for investigation of hydrogen bonding.

The power of this technique will be illustrated here on the example of dehydrogenation of ammonia borane, where IR spectroscopy, gives a unique insight and shed a light into important, but previously oversought mechanistic aspects.



***Surface processes***

---



# THEORETICAL ANALYSIS OF ADSORPTION PROPERTIES OF DOPED HEXAGONAL MgO NANOTUBES

Aleksandar Z. Jovanović

*University of Belgrade, Faculty of Physical Chemistry, Studentski trg 12-16, 11158  
Belgrade, Serbia*

Oxide materials have a wide range of application in various fields of technology. Oxides exhibit diverse electronic and crystalline structures, and some can behave as insulators, others as semiconductors, while some have the conductive properties similar to those of metals. MgO is one of the oxides whose properties are being intensively studied. Due to its availability, ease of preparation, stability and chemical inertness, it can be used in investigating adsorption, as a catalyst support, or it can be functionalized by introducing defects or impurities into its structure.

Here we will show the results of DFT calculations of the properties of hexagonal MgO nanotubes of varying sizes. Properties of the nanotubes were altered by creating a vacancy and subsequently introducing an Li atom at Mg vacancies, or B, C, N, or F atoms at O vacancies, at different sites along the nanotube. Change of electronic structure and the induction of magnetization at the dopant site points towards the possible use of these systems as adsorbents or catalysts, or as new types of magnetic materials. Adsorption properties are tested using CO as a probe molecule. It is shown that adsorption properties are drastically changed at and around the dopant sites, the change being localized on the surrounding atoms.

## CHANGING REACTIVITY OF SUPPORTED METAL ATOMS BY SUBSTRATE DOPING – THE CASE OF Pd AND Au ON DOPED MgO(001)

Igor A. Pašti<sup>1</sup>, Natalia V. Skorodumova<sup>2,3</sup>

*<sup>1</sup>University of Belgrade, Faculty of Physical Chemistry, Studentski trg 12-16, 11158 Belgrade, Serbia; <sup>2</sup>Department of Physics and Astronomy, Uppsala University, Box 516, 751 20 Uppsala, Sweden; <sup>3</sup>Materials Science and Engineering, KTH - Royal Institute of Technology, Brinellvägen 23, 100 44 Stockholm, Sweden*

Supported metal catalysts play important role in many contemporary technologies. By dispersing the catalyst over suitable support one increases its specific surface and the number of active sites, resulting with more economical catalytic material. The upper limit of catalyst dispersion is, naturally, single atom on the support in which case, ideally, each metal atom could provide catalytic activity. Oxide materials, such as MgO, are often used as catalyst supports as being chemically inert and thermally stable. In our previous work [1] we have used density functional theory calculations and showed that electronic, magnetic and chemical properties of MgO(001) surface are significantly modified by substitutional doping with B, C and N. Here we extend mentioned work and analyze what are the effects of doping of MgO(001) on its metal-supporting performance and how the presence of dopants affects the reactivity of supported metal atoms. We have found that B, C and N surface impurities could potentially serve as strong anchoring sites for Pd and Au atoms (**Fig. 1**), which are very mobile on pristine MgO(001). Pd and Au adsorption energies are much higher at impurity sites, compared to adsorption energies on pristine MgO terrace sites, leading us to conclude that mobility of Au and Pd monomers will be reduced on doped MgO. Reactivity of supported Au and Pd atoms on doped MgO(001) was probed using CO and it was found that it is different from that found for metals on pure MgO(001). In this sense supported Au and Pd atoms differ to a great extent. When Pd is adsorbed on impurity sites, it binds CO much weaker than Pd monomer at pure MgO(001). If Pd monomer is far from the impurity site its affinity towards CO is similar to that of Pd on pure MgO(001). However, when Au is adsorbed on impurity site it tends to bind CO stronger than Au monomer on pure MgO(001). The effect increases from B to N. In contrast to Pd case, the effects of the impurities on the reactivity of supported Au monomers seem to be somewhat longer-ranged: increased reactivity is observed also for Au monomers adsorbed on the next nearest neighbours (oxygen) sites of the dopant site on MgO(001). Here we also see that the effect is the most prominent in the case of N-doped MgO(001).

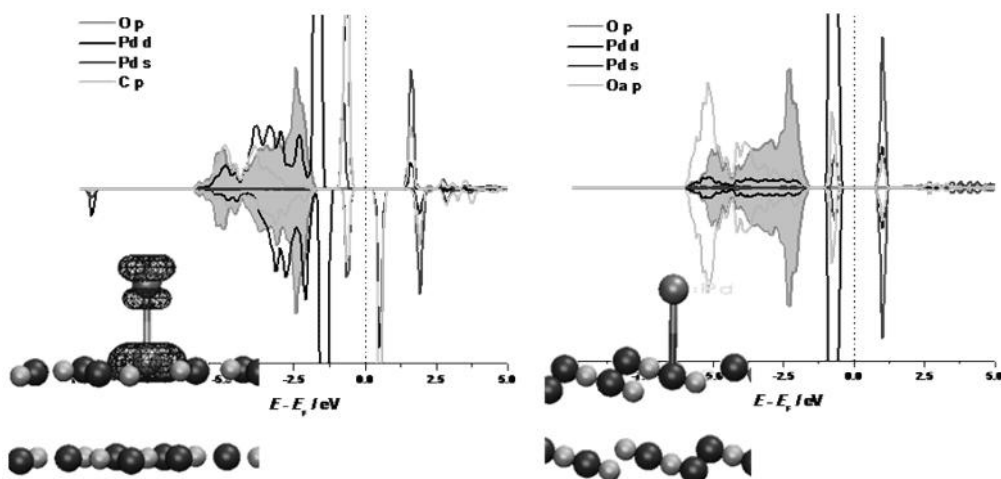


**Fig. 1.** Projected density of states of Pd supported by C-doped MgO(001) (left) and pristine MgO(001) (right).

#### Acknowledgement

This work was supported by the Swedish Research Links initiative of the Swedish Research Council (348-2012-6196). Computational resources are provided by the Swedish National Infrastructure for Computing (SNIC).

#### References

- [1] I.A. Pašti, N.V. Skorodumova, *Phys. Chem. Chem. Phys.*, 2016, **18**(1), 426-435.

# MODIFYING THE SURFACE OF NITROGEN-DOPED TiO<sub>2</sub> PHOTOCATALYST WITH PALLADIUM AND PLATINUM

Katarina Batalović<sup>1</sup>, Igor Pašti<sup>2</sup>, Jana Radaković<sup>1</sup>, Carmen Rangel<sup>3</sup>

<sup>1</sup>VINCA Institute of nuclear sciences, University of Belgrade, P. O. Box 522, 11001 Belgrade, Serbia; <sup>2</sup>Faculty of physical chemistry, University of Belgrade, Studentski trg 12-16, 11000 Belgrade, Serbia; <sup>3</sup>LNEG I.P., Estrada do Paço do Lumiar, 22, 1649-038 Lisboa, Portugal Lisbon, Portugal

Titanium dioxide is considered to be promising, cheap and easily accessible photocatalysts for environmental-friendly energy solutions [1]. Main drawbacks of TiO<sub>2</sub> are its poor visible light absorption and fast recombination of photo-generated electron/hole pairs [1,2]. Doping bulk TiO<sub>2</sub> with nitrogen, boron, phosphorus and some other non-metals was shown to significantly improve visible light activity [2]. Recently, co-doping with more than one element is used as new approach to the design of desirable photocatalyst. Here, we pay attention to synergism between nitrogen doping and surface modification of nanostructured TiO<sub>2</sub>, by photodeposition of platinum and palladium at the surface.

Experimental investigation of nanosized nitrogen-doped anatase TiO<sub>2</sub>, Pt/N-TiO<sub>2</sub> and Pd/N-TiO<sub>2</sub> confirmed significant improvement of optical properties compared to the pure anatase, as well as specific behavior of noble metals at the surface. Calculations based on density functional theory are used to explain some experimental findings and study the surface structure and energetic of platinum and palladium deposition on 001 surface of nitrogen-doped anatase TiO<sub>2</sub>. To address the location of nitrogen atom in the anatase cell, and obtain energy of the N 1s electronic level in case of interstitial and substitutional nitrogen in anatase TiO<sub>2</sub>, we performed electronic structure calculations on bulk nitrogen doped anatase using full potential APW+lo method and Slater's transition state approximation. Further, using pseudopotential method, the location of nitrogen at the 001 surface is found to be the more stable than sub-surface ones, and energetic and structure of noble metal deposition at this surface is studied. Clustering of metal particles at the surface is also addressed, and electronic structure of Pt/N-TiO<sub>2</sub> and Pd/N-TiO<sub>2</sub> is examined, to explain observed improvement in optical properties due to metal deposition.

## References

- [1] M. Ni, M.K.H. Leung, D.Y.C. Leung, K. Sumathy, *Renew. Sust. Energy Rev.*, 2007,**11**, 401-425.
- [2] J. Li, N. Wu, *Catal. Sci. Technol.* 2015, **5**, 1360-1384.



# SURFACE MODIFICATION BY SELF-ASSEMBLED MONOLAYERS OF FLUORESCENT DYES

Aleksandra Marković\*, Gunther Wittstock

*University of Oldenburg, Faculty of Mathematic and Sciences, Physical Chemistry,  
D-26111 Oldenburg, Germany (\*[aleksandra.markovic1@uni-oldenburg.de](mailto:aleksandra.markovic1@uni-oldenburg.de))*

Surfaces can be modified by self-assembly of organic molecules. Molecules are chemisorbed on the surface by "head groups", for which thiols or silanes are suitable for gold or glass surfaces [1].

Here we aim to assemble derivatives of diaminoterephthalic acid on a gold surface in mixed self-assembled monolayers. Diaminoterephthalic acid derivatives have been synthesized as fluorescent dyes by Wallisch and Christoffers [2]. Some derivatives are turn-on probes, e.g. they emit fluorescence only when bound to an effector [3] which facilitates the distinction of reacted vs. unreacted dye.

Dyes based on diaminoterephthalic acid can have thiol groups on alkane side chain. Dyes with this structure can be assembled on surfaces by self assembly techniques and monolayers can be diluted with corresponding alkanes. Surfaces build in this way are electrochemically active and were characterised by cyclic voltammetry in different solvents. By electrochemical reaction these surfaces can be activated to bind different objects such as nanoparticles, proteins by 1-4 addition reactions to the oxidized form [4]. Those changes can be examined by fluorescence spectroscopy. Dyes based on diaminoterephthalates change their emission wavelength depending on the occupation of binding sites.

## References

- [1] A. Ulman, Chem. Rev., 1996, **96**, 1533-1554.
- [2] M. Wallisch, J. Christoffers, Diaminoterephthalic acid derivatives – Fluorescent dyes for life sciences.
- [3] L. Freimuth, J. Christoffers, Chem. Eur. J., 2015, **21**, 1 – 9.
- [4] M. Shamsipur, H. S. Kazemi, A. Alizadeh, F. M. Mousavi, M. S. Workentin, J. Electroan. Chem., 2007, **610**, 218 – 226.

## PHYSICS AND CHEMISTRY ON-SURFACES: INTERFACE MATERIALS CREATED VIA SURFACE ENGINEERING

M. Baljozovic<sup>1\*</sup>, J. Girovsky<sup>1</sup>, J. Nowakowski<sup>1</sup>, Md. Ehesan Ali<sup>2,3</sup>,  
H. R. Rossmann<sup>1</sup>, T. Nijs<sup>4</sup>, E. Aeby<sup>4</sup>, S. Nowakowska<sup>4</sup>, D. Siewert<sup>4</sup>, G. Srivastava<sup>1</sup>,  
C. Wäckerlin<sup>5</sup>, J. Dreiser<sup>6</sup>, S. Decurtins<sup>7</sup>, Shi-Xia Liu<sup>7</sup>, P. M. Oppeneer<sup>3</sup>,  
T. A. Jung<sup>1</sup>, N. Ballav<sup>8</sup>

<sup>1</sup>Laboratory for Micro- and Nanotechnology, Paul Scherrer Institute, Switzerland ([\\*milos.baljozovic@psi.ch](mailto:milos.baljozovic@psi.ch)); <sup>2</sup>Institute of Nano Science and Technology-Mohali, Habitat Centre, India; <sup>3</sup>Department of Physics and Astronomy, Uppsala University, Sweden; <sup>4</sup>Department of Physics, University of Basel, Switzerland; <sup>5</sup>Institute of Condensed Matter Physics, École Polytechnique Fédérale de Lausanne, Switzerland; <sup>6</sup>Swiss Light Source, Paul Scherrer Institute, Switzerland; <sup>7</sup>Departement für Chemie und Biochemie, Universität Bern, Switzerland; <sup>8</sup>Department of Chemistry, Indian Institute of Science Education and Research (IISER), India

Surface science is focused on the study of physical and chemical properties of interfaces in general. Of particular interest are phenomena that are emerging from the reduced dimensionality of the interfaces. For many decades there has been a growing interest in surface science. There are many publications appearing each year which cover fundamentally important questions and/or refer to a broad range of practical applications including heterogeneous catalysis, semiconductor device fabrication, fuel cells, self-assembled monolayers, adhesives and many others.

The task of tuning physicochemical properties of interfaces via surface engineering represents the main topic of this contribution. It is achieved by i) functionalizing a metallic surface with adsorbate-induced superstructures, ii) directing the assembly of surface-supported molecules and/or iii) by subtle modifications of the adsorbed organic molecules. Investigation of these modifications are performed in Ultra-High Vacuum (UHV) conditions using Surface sensitive techniques which provide information on the atomic composition and structure: X-ray Photoemission Spectroscopy (XPS) and X-ray Absorption Spectroscopy (XAS) provide surface chemical composition; X-ray Magnetic Circular Dichroism (XMCD) provides species dependent magnetic properties; Low-Energy Electron Diffraction (LEED) and Scanning Tunnelling Microscopy/Spectroscopy (STM/S) reveal structural information while the latter technique also provides the means to perform local experiments about surface electronic states and surface forces. The experimental results are complemented by Density Functional Theory (DFT) calculations performed by collaborators from Uppsala University (Sweden).

# ON THE ORIGIN OF SURPRISING ATTRACTIVE INTERACTIONS BETWEEN ELECTRONEGATIVE OXYGEN ADATOMS ON ALUMINUM SURFACES

Matic Poberžnik, Anton Kokalj

*Department of Physical and Organic Chemistry, Jožef Stefan Institute, Ljubljana, Slovenia*

When electronegative atoms adsorb on a electropositive metal surface, charge transfer occurs and the adatoms become negatively charged. Because of this charge accumulation, repulsive lateral interactions are expected between them. According to the classical method of images the lateral repulsion between negatively charged adatoms can be treated as a dipole-dipole interaction that scales as  $\Theta^3/2$ , where  $\Theta$  is the surface coverage of adatoms. Such dependence is typical for chemisorbed atomic oxygen on transition metal surfaces (**Fig. 1a** shows the example of O @ Cu(111)). However, in the case of O on Al(111) and Al(100) surfaces the opposite occurs and the binding energy magnitude increases with increasing coverage (see **Fig. 1b**). Although this anomaly has been noticed,<sup>1,2</sup> no sound explanation as to why this occurs has been given in the literature. Hence, we attempted to explain this anomaly on a molecular level by means of DFT calculations. We found that the attractive interactions are a consequence of a simple electrostatic stabilization. Namely, at full monolayer coverage the O adatoms are located close to the surface and together with positively charged surface Al atoms form an interlaced layer of anions and cations, which is electrostatically stable (**Fig. 1c** shows the charge density difference of 1 ML O @ Al(111); note the alternation of electron charge excess and deficit regions). We conclude that the attractive interactions between negatively charged O adatoms at high-coverage stem from an interplay between Coulombic interactions and geometric effects, which depend on the height of adatoms, i.e., there exists a critical adatom height below which the lateral interactions are attractive and above which they are repulsive.

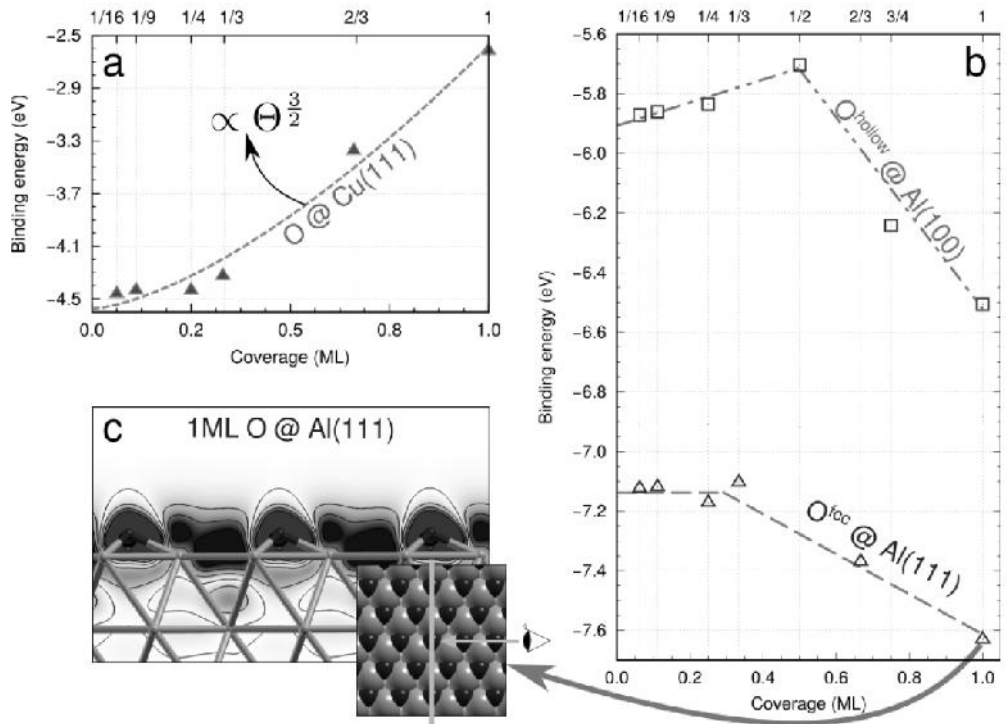


**Fig. 1.** Binding energy of oxygen on (a) Cu(111) and (b) Al(111) and Al(100) with respect to coverage ( $\Theta$ ). (c) Charge density difference of 1 ML O @ Al(111); blue (red) color corresponds to electron charge deficit (excess) regions.

#### References

- [1] J. Jacobsen, B. Hammer, K.W. Jacobsen and J.K. Norskov, Phys. Rev. B 1995, **52**, 14954.
- [2] A. Kiejna, B.I. Lundqvist, Phys. Rev. B 2001, **63**, 1.

## KINETICS OF WATER ADSORPTION ON THE RUTILE $\text{TiO}_2(110)$ SURFACE

Johan O. Nilsson<sup>1</sup>, Mikael Leetmaa<sup>1</sup>, Baochang Wang<sup>2</sup>, Pjotr Zguns<sup>3</sup>,  
Anders Sandell<sup>3</sup>, Natalia V. Skorodumova<sup>1, 3</sup>

<sup>1</sup>*Department of Materials Science and Engineering,  
KTH - Royal Institute of Technology, Brinellvägen 23, 100 44 Stockholm, Sweden;*

<sup>2</sup>*Department of Physics and the Competence Centre for Catalysis,  
Chalmers University of Technology, 412 96, Sweden;* <sup>3</sup>*Department of Physics and  
Astronomy, Uppsala University, Box 516, 751 20 Uppsala, Sweden*

Titanium dioxide,  $\text{TiO}_2$ , has a wide range of technological applications within for example the fields of photovoltaics, (photo-)catalysis, and gas sensing. In such applications chemical agents react with stable surfaces of  $\text{TiO}_2$ . In particular, the interactions involving water molecules and the surfaces of  $\text{TiO}_2$  have received an overwhelming attention, in both experimental and theoretical studies alike. Nevertheless, even the most fundamental aspects of water-titania interaction are not fully understood yet. Here we investigate the kinetics of adsorption, diffusion and dissociation of water on the rutile  $\text{TiO}_2(110)$  surface using density functional methods (DFT) with different exchange-correlation (XC) functionals. Using Kinetic Monte Carlo simulations based on the DFT barriers, we demonstrate how the choice of the XC functional radically changes the dynamics of the simulated water-titania system.



***General session***

---





## NANO-IMPACTS: NEW INSIGHTS INTO NANOPARTICLES

Richard G. Compton

*Department of Chemistry, Physical and Theoretical Chemistry Laboratory, Oxford University, South Parks Road, Oxford OX1 3QZ, U.K.*

Some recent progress in the electrochemical study of single nanoparticles by means of the nano-impacts approach will be briefly surveyed and evaluated. [1-5]

Experiments with diverse types of nanoparticles will be reported including the sizing and characterisation of metallic (Ag, Ni) and metal oxides ( $\text{Fe}_3\text{O}_4$ ) and the measurement of their concentrations. The application to core-shell structures will be described along with the use of impacts for assessing the extent of doping of organic (TCNQ) and polymeric (poly-N-vinylcarbazole) nanoparticles.

Electro-catalytic processes occurring during nano-impacts of soft nanoparticles will be discussed with reference to the reduction of oxygen mediated via attomole quantities of vitamin B12 present in single nano-droplets.

Finally nano-impacts of super-paramagnetic nanoparticles in the presence and absence of magnetic fields will be discussed.

### References

- [1] Y. Zhou, N.V. Rees, R.G. Compton, *Angew. Chem.* 2011, **50**, 4219-4223.
- [2] W. Cheng, X. Zhou, R.G. Compton, *Angew. Chem.* 2013, **52**, 12980-12984.
- [3] X. Zhou, W. Cheng, R.G. Compton, *Angew. Chem.* 2014, **53**, 12587-12589.
- [4] W. Cheng, R. G. Compton, *Angew. Chem.* 2015, **54**, 7082-7085.
- [5] L.R. Holt, B.J. Plowman, N.P. Young, K. Tschulik, R.G. Compton, *Angew. Chem.* 2016, **55**, 397-400.

## 4D PHASE DIAGRAMS FOR THE MOLTEN SALT REACTOR MATERIALS

V. Lutsyk<sup>1,2\*</sup>, V. Vorob'eva<sup>1</sup>

<sup>1</sup>*Institute of Physical Materials Science, 6 Sahyanova st., 670047 Ulan-Ude, Russia*  
(\*[vluts@ipms.bscnet.ru](mailto:vluts@ipms.bscnet.ru)), <sup>2</sup>*Buryat State University, 24a Smolin st.,*  
*670000 Ulan-Ude, Russia*

Fluorides of metals with the small neutron-capture cross section usually compose the basis of fuel compositions for the molten-salt nuclear reactors of IV generation. Chloride systems, comparing with them, have higher pressures of vapor and low stability at high temperatures. They are less aggressive with respect to the structure of material and have lower melting points. Therefore for guaranteeing the more reliable operation of the new reactors it is worthwhile to examine chemical processes and equilibria precisely in the reciprocal fluoride-chloride systems, using for the polyhedration special algorithms [1].

It is possible to say that all fluoride systems, which form ternary systems  $M_1, M_2, U(Pu) || F$  ( $M_1, M_2 = Li, Na, K, Rb$ ), are more or less in detail experimentally studied, comprised of fluorides or chlorides of alkali metals and uranium (plutonium). But the chloride systems  $M_1, M_2, U(Pu) || Cl$  ( $M_1, M_2 = Li, Na, K, Rb$ ) are less studied. And entirely there is no information about the ternary reciprocal systems  $M, U(Pu) || F, Cl$  ( $M = Li, Na, K, Rb$ ). Accordingly, polyhedration of quaternary reciprocal systems  $M_1, M_2, U(Pu) || F, Cl$  ( $M_1, M_2 = Li, Na, K, Rb$ ) can be only multivariant, and the design of 4D computer models of T-x-y-z diagrams of the obtained systems can be only virtual.

E.g., it is possible to say about systems, forming  $Li, Na, U || F, Cl$  [2-5]:  $LiF-NaF$ ,  $NaF-NaCl$ ,  $LiF-LiCl$  are eutectic;  $LiCl-NaCl$  has continuous series of solid solutions;  $UF_4-UCl_3$  has incongruent compounds  $2UCl_3 \cdot UF_4$ ,  $UCl_3 \cdot 7UF_4$ ;  $LiF-UF_4$  has an eutectic, 3 peritectics and incongruent compounds  $4LiF \cdot UF_4$ ,  $7LiF \cdot 6UF_4$ ,  $LiF \cdot 4UF_4$  [4, p. 85];  $NaF-UF_4$  has 3 eutectics, 2 peritectics, congruent ( $4NaF \cdot UF_4$ ,  $7NaF \cdot 6UF_4$ ) and incongruent ( $2NaF \cdot UF_4$ ,  $5NaF \cdot 3UF_4$ ) compounds [4, p. 88];  $LiCl-UCl_3$  [4, p. 131] and  $NaCl-UCl_3$  [4, p. 133] has an eutectic. The data about systems  $LiF-NaF-UF_4$  and  $LiCl-NaCl-UCl_3$  are absent. As  $LiF-NaCl$  is eutectic [5], it means that the diagonal  $LiF-NaCl$  is stable in the system  $Li, Na || F, Cl$ . The data about reciprocal systems  $Li, U || F, Cl$  и  $Na, U || F, Cl$  are absent. Hence it is possible to divide system  $Li, Na, U || F, Cl$  (**Fig. 1**). Since the diagonal  $LiF-NaCl$  is stable and compounds  $R1=3NaF \cdot UF_4$ ,  $R2=7NaF \cdot 6UF_4$  are congruent, then 2 variants of polyhedration with diagonal  $LiF-UCl_3$  (**Fig. 1a-1b**) and 2 versions with diagonal  $LiCl-UF_4$  (**Fig. 1c-1d**) are considered. Moreover the last version (**Fig. 1d**) is impossibl. Thus, 5 tetrahedra ( $LiF-NaF-NaCl-R1$ ,  $LiF-UF_4-NaCl-UCl_3$ ,  $LiF-UF_4-$

NaCl-R2, LiF-LiCl-NaCl-UCl<sub>3</sub>, LiF-NaCl-R1-R2) are obtained in the first variant with the inner diagonal LiF-UCl<sub>3</sub> and 3 diagonals from the vertex NaCl (**Fig. 1a**).

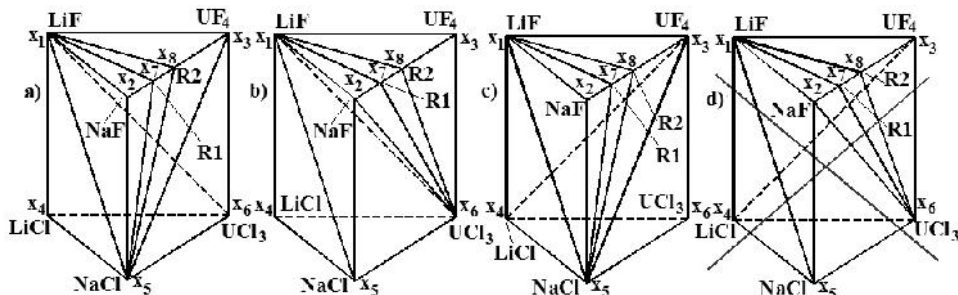


**Fig. 1.** Polyhedration variants of the system Li,Na,U||F,Cl with compounds 3NaF·UF<sub>4</sub>, 7NaF·6UF<sub>4</sub> (with stable diagonal UF<sub>4</sub>-UCl<sub>3</sub> in the system U<sup>3+</sup>,U<sup>4+</sup>||F,Cl)

Second variant of polyhedration with the stable diagonal LiF-UCl<sub>3</sub> and 3 diagonals from the vertex UCl<sub>3</sub> (**Fig. 1b**) gives also 5 tetrahedra (LiF-LiCl-NaCl-UCl<sub>3</sub>, LiF-UCl<sub>3</sub>-R1-R2, LiF-NaF-NaCl-UCl<sub>3</sub>, LiF-NaF-UCl<sub>3</sub>-R1, LiF-UF<sub>4</sub>-UCl<sub>3</sub>-R2). If the diagonal LiCl-UF<sub>4</sub> is stable, that the only variant with 3 stable diagonals from the vertex NaCl is possible (**Fig. 1c**). This case gives 5 tetrahedra (LiF-NaF-NaCl-R1, LiF-UF<sub>4</sub>-LiCl-NaCl, LiF-UF<sub>4</sub>-NaCl-R2, LiF-NaCl-R1-R2, UF<sub>4</sub>-LiCl-NaCl-UCl<sub>3</sub>).

Among the enumerated 15 tetrahedra the tetrahedron  $x_1x_4x_5x_6$  (LiF-LiCl-NaCl-UCl<sub>3</sub>) is encountered twice in the first and second versions. Tetrahedra  $x_1x_2x_5x_7$ ,  $x_1x_3x_5x_8$ ,  $x_1x_5x_7x_8$  are repeated twice in the first and third versions. Hence, it is necessary to examine 11 quaternary subsystems: all 5 from the first variant, 4 from second (without  $x_1x_4x_5x_6$ ) and 2 from third (without  $x_1x_2x_5x_7$ ,  $x_1x_3x_5x_8$ ,  $x_1x_5x_7x_8$ ). If further to assume that diagonals, accepted as the stable in all 3 variants, are eutectic, then the system LiF-LiCl-NaCl-UCl<sub>3</sub> is formed by 5 eutectic systems and 1 (LiCl-NaCl) with continuous series of solid solutions (**Fig. 2a**). Analogously, systems LiF-NaF-NaCl-R1, LiF-NaF-NaCl-UCl<sub>3</sub> and LiF-NaF-UCl<sub>3</sub>-R1 are formed by 6 binary and 4 ternary eutectic systems (**Fig. 2b**). Tetrahedron  $x_1x_5x_7x_8$  (LiF-NaCl-R1-R2 with R1=3NaF·UF<sub>4</sub>, R2=7NaF·6UF<sub>4</sub>) is complicated by the subsystem  $x_7x_8$  (R1-R2) of the binary system NaF-UF<sub>4</sub> with incongruent compounds R3=5NaF·3UF<sub>4</sub>, R4=2NaF·UF<sub>4</sub> [4, p. 88] (**Fig. 2c**). Hence quasi-peritectic Q<sub>1</sub>: L+R2→LiF+R3, Q<sub>2</sub>: L+R3→LiF+R4 or Q<sub>3</sub>: L+R2→NaCl+R3, Q<sub>4</sub>: L+R3→NaCl+R4 and eutectic E<sub>3</sub>: L→LiF+R1+R4 or E<sub>4</sub>: L→NaCl+R1+R4 reactions occur in the appropriate ternary systems with LiF and NaCl. These invariant transformations and eutectic reactions E<sub>1</sub>: L→LiF+NaCl+R1, E<sub>2</sub>: L→LiF+NaCl+R2 in other ternary systems make it possible to expect quasi-peritectic  $\pi_1$ : L+R2→LiF+NaCl+R3,  $\pi_2$ : L+R3→LiF+NaCl+R4 and eutectic  $\varepsilon$ : L→LiF+NaCl+R1+R4 reactions. It is analogously arranged the subsystem LiF-UF<sub>4</sub>-NaCl-R2 (R2=7NaF·6UF<sub>4</sub>) with

incongruent compounds  $R5=4LiF \cdot UF_4$ ,  $R6=7LiF \cdot 6UF_4$ ,  $R7=LiF \cdot 4UF_4$  [4, p. 85]. Accordingly, 3 quasi-peritectic reactions occur in ternary systems with NaCl or with R2. They lead to 1 eutectic and 3 quasi-peritectic reactions in the quaternary system (**Fig. 2d**).

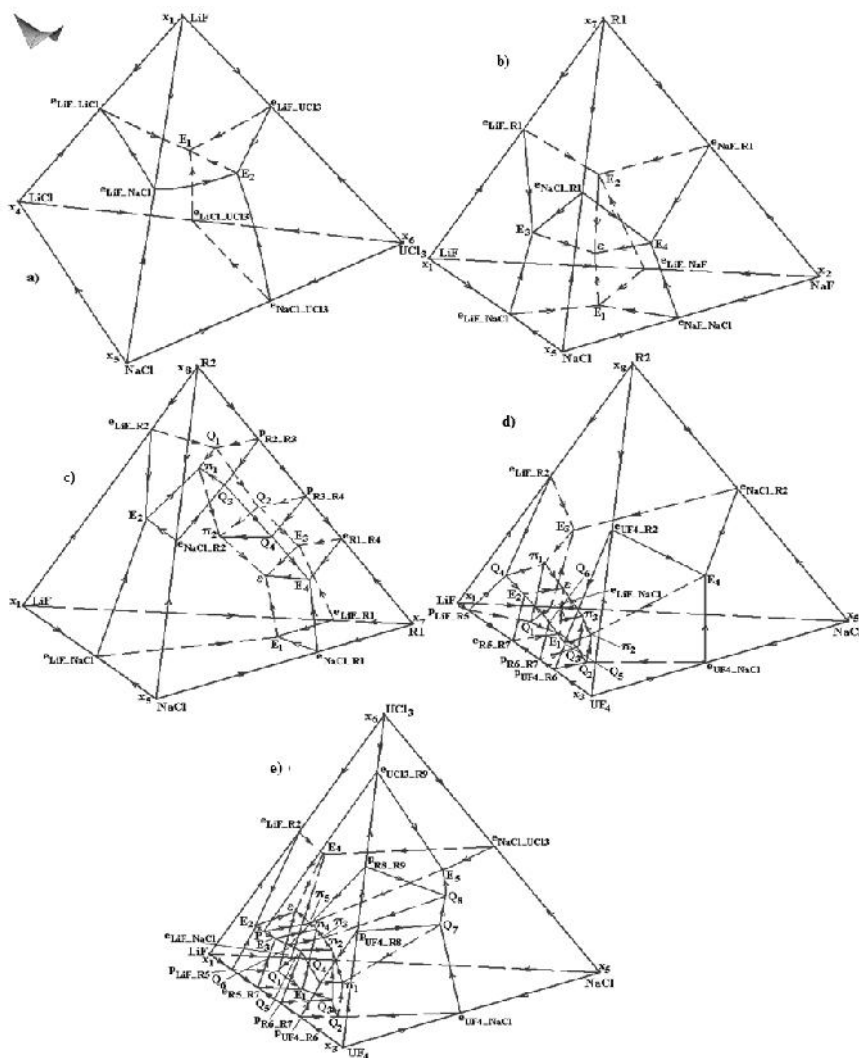


**Fig. 2.** First variant polyhedration of the system Li,Na,U||F,Cl (**Fig. 1a**): LiF-LiCl-NaCl-UCl<sub>3</sub> (a), LiF-NaF-NaCl-R1 (3NaF·UF<sub>4</sub>) (b), LiF-NaCl-R1(3NaF·UF<sub>4</sub>)-R2 (7NaF·6UF<sub>4</sub>) (c), LiF-UF<sub>4</sub>-NaCl-R2 (7NaF·6UF<sub>4</sub>) (d), LiF-UF<sub>4</sub>-NaCl-UCl<sub>3</sub> (e)

Subsystem LiF-UF<sub>4</sub>-NaCl-UCl<sub>3</sub> is the most complex. Only one ternary system LiF-NaCl-UCl<sub>3</sub> is eutectic (**Fig. 2e**). System UF<sub>4</sub>-NaCl-UCl<sub>3</sub> is similar to LiF-R1-R2, the forming it binary system UF<sub>4</sub>-UCl<sub>3</sub> has also 2 incongruent compounds

$R8=7UF_4 \cdot UCl_3$ ,  $R9=UF_4 \cdot 2UCl_3$ . System  $LiF-UF_4-NaCl$  with 3 incongruent compounds has already considered as boundary of the system  $LiF-UF_4-NaCl-R2$  (**Fig. 2d**). Ternary system  $LiF-UF_4-UCl_3$  is the most complex. It is formed by  $LiF-UF_4$  with  $R5, R6, R7$  and  $UF_4-UCl_3$  with  $R8, R9$  incongruent compounds. Possible chain of invariant equilibria consists of quasi-peritectic ( $Q_4, Q_5, Q_6$ ), peritectic ( $P$ ) and eutectic ( $E_2, E_3$ ) reactions. Taking into account all invariant transformations in 4 boundary ternary systems  $E_1-E_5, P, Q_1-Q_8$  it is most probable the quaternary system phase reactions scheme with 5 invariant 5-phase reactions.

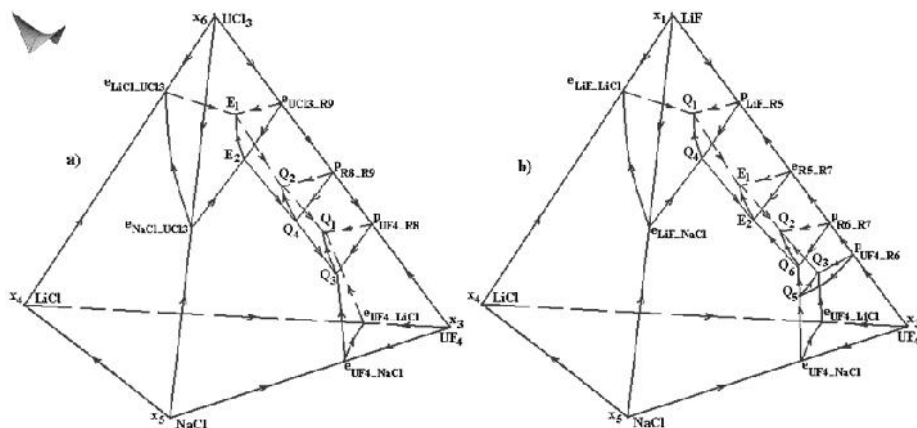


**Fig. 3.** Subsystems  $UF_4-LiCl-NaCl-UCl_3$  (a),  $LiF-UF_4-LiCl-NaCl$  (b) are results of the third variant (**Fig. 1c**) polyhedration of the system  $Li, Na, U|F, Cl$ .

Two ( $LiF-NaF-NaCl-UCl_3$  and  $LiF-NaF-UCl_3-R1$ ) of 5 tetrahedra, obtained by the second variant polyhedration, besides the coinciding with the first variant  $x_1x_4x_5x_6$  (subsystem  $LiF-LiCl-NaCl-UCl_3$  with 5 binary eutectic systems and 1 with continuous series of solid solutions), are subsystems of eutectic type. The geometric structure of remaining subsystems  $LiF-UCl_3-R1-R2$  and  $LiF-UF_4-UCl_3-R2$  is similar to the appropriate subsystems  $LiF-NaCl-R1-R2$  and  $LiF-UF_4-NaCl-UCl_3$  of the first polyhedration variant.

As for the tetrahedra list, obtained in the third variant, subsystems  $LiF-NaF-NaCl-R1$ ,  $LiF-NaCl-R1-R2$ ,  $LiF-UF_3-NaCl-R2$  coincide with the appropriate tetrahedra of the first variants (**Fig. 3b-3d**). Remaining subsystems  $UF_4-LiCl-NaCl-UCl_3$  and  $LiF-UF_4-LiCl-NaCl$  are topologically equivalent to subsystems  $LiF-NaCl-R1-R2$  (**Fig. 3b**) and  $LiF-UF_4-NaCl-R2$  (**Fig. 3c**), with exception of the fact that corresponding subsystems of the third variant are formed by the binary system  $LiCl-NaCl$  with continuous solid solutions, and therefore places of eutectic ternary systems are occupied by systems with univariant eutectic interaction of  $UCl_3$  (**Fig. 3a**) or  $LiF$  (**Fig. 3b**) with the solid solution  $LiCl(NaCl)$ . Furthermore, invariant 5-phase transformations are absent in these subsystems.

### Acknowledgement

This work has been performed under the program of fundamental research SB RAS (project 0336-2014-0003) and was partially supported by the Russian Foundation for Basic Research (projects 14-08-00453, 15-43-04304).

### References

- [1] V.I. Lutsyk, V.P. Vorobeve, *Rus. J. Inorgan. Chem.*, 2014, **59**, 956-970.
- [2] M. Malinovsky, J. Gabcova, *Chem. Papers*, 1976, **30**, 783-795.
- [3] O. Lushchnikova, E. Frolov, *et al.*, *Rus. J. Inorg. Chem.*, 2013, **58**, 102-106.
- [4] R.E. Thoma, Editor. *Phase Diagrams of Nuclear Reactor Materials*, Union Carbide Corp., Oak Ridge, Tennessee, 1959, 205.
- [5] J. Gabcova, J. Peschl, *et al.*, *Chem. Papers*, 1976, **30**, 796-804.

# NEAR-WALL HINDERED DIFFUSION IN CONVECTIVE SYSTEMS: TRANSPORT LIMITATIONS IN COLLOIDAL AND NANOPARTICULATE SYSTEMS

Stanislav V. Sokolov, Enno Kätelhön, Richard G. Compton

*Department of Chemistry, Physical and Theoretical Chemistry Laboratory, Oxford  
University, South Parks Road, Oxford OX1 3QZ, U.K.*

Development of renewable energy sources requires cheap and efficient ways of generating and storing energy. Redox flow fuel cell (RFFC) technology is an attractive option due to decoupled power/energy storage design and potential scalability for a wide range of industrial uses. Novel redox flow fuel cells designs involve the use of colloidal suspensions of electroactive nanoparticles used as ‘electrofuels’ in order to increase the energy density and capacity of such systems under conditions of forced convection. [1,2]

The hydrodynamic-diffusive behaviour of the nanoparticles is different to molecular species traditionally used in redox-flow fuel cells due to the inherently larger radius of the particles and is likely to have a significant impact on the resultant current response. Particles are known to experience near-wall hindered diffusion as they approach a solid boundary, leading to an apparent reduction of the diffusion coefficient.[3] Hence efficient, rational design of the next generation of RFFCs requires understanding of the mass transport as it involves a complex interplay between convection and diffusion.

The rotating disk electrode (RDE) is commonly employed in fuel cell testing and provides a suitable system for theoretical investigation due to a particular advantage of laminar flow and is used as a model system in the present work. Through numerical simulation we demonstrate significant effect of near-wall hindered diffusion on the current response at high overpotentials and fast rotation rates. Under such conditions near-wall hindered diffusion plays a significant role and leads to lower limiting currents and deviations from linearity in so-called “Levich” plots observed for molecular species and limits the practical efficiency.[4]

## References

- [1] S. Sen, E.V. Timofeeva, C.J. Pelliccione, J.P. Katsoudas, D. Singh, C.U. Segre, ECS Meet. Abstr., 2015, MA2015-01(1), 224.
- [2] S. Sen, E. Moazzen, S. Aryal, C.U. Segre, E.V. Timofeeva, J. Nanoparticle Res., 2015, **17**(11), 437–445.
- [3] H. Brenner, Chem. Eng. Sci., 1961, **16**(3–4), 242–251.
- [4] S. V. Sokolov, E. Kätelhön, R.G. Compton, J. Phys. Chem. C, 2016, **120**(19), 10629–10640.

# MANUFACTURING POLYMERIC CAPSULES FOR CO<sub>2</sub> CAPTURE USING MICROFLUIDIC EMULSIFICATION AND ON-THE-FLY PHOTOPOLYMERISATION

Seyed Ali Nabavi<sup>1,2</sup>, Goran T. Vladislavljević<sup>1\*</sup>, Vasilije Manović<sup>2</sup>

<sup>1</sup>*Loughborough University, Loughborough, LE11 3TU, UK;* <sup>2</sup>*Cranfield University, Cranfield, MK43 0AL, UK* (\*[G.Vladislavljevic@lboro.ac.uk](mailto:G.Vladislavljevic@lboro.ac.uk))

## Introduction

In this work, novel monodispersed polymeric core/shell microcapsules of controllable size and shell thickness have been developed and produced using continuous microfluidic emulsification and “on-the-fly” photopolymerisation. The process can be used for gas capture or sensing and allows encapsulation of CO<sub>2</sub> selective liquid with 100% efficiency inside a semipermeable shell. Conventional methods for fabrication of core/shell capsules such as internal phase separation, interfacial polymerization, complex coacervation and layer-by-layer electrostatic deposition require multi-stage processing and do not permit precise control over the shell thickness and capsule size.

The process was used to encapsulate aqueous solutions of K<sub>2</sub>CO<sub>3</sub> of various concentrations in the presence of the pH-sensitive dye m-cresol purple, so that CO<sub>2</sub> adsorption can be visualised (**Fig. 1a**). Post-combustion amine scrubbing, mainly using monoethanolamine (MEA), is the most established commercial technology for CO<sub>2</sub> capture from large point sources. Although MEA exhibits a high CO<sub>2</sub> selectivity and capture capacity, it is a corrosive and volatile liquid, and requires a high regeneration energy [1]. On the other hand, solid adsorbents, such as zeolites, metal-organic frameworks, and activated carbons are non-volatile, noncorrosive materials and have the lower regeneration energy than amines. However, they suffer from low CO<sub>2</sub> capture capacity and selectivity, especially at low pressures [2]. Our core/shell capsules are hybrid liquid/solid materials that keep all benefits of liquid absorbents, such as high CO<sub>2</sub> capture capacity and selectivity, while providing protection against evaporation and a high surface area to volume ratio of solid adsorbents, up to 100 times higher than in a typical packed-bed column [3].

## Experimental

Core/shell droplets have been produced using a glass capillary microfluidic device that combines co-flow and counter-current flow focusing [4] (**Fig. 1b**) placed on the stage of an inverted microscope with a high-speed camera attached to it. The microfluidic device was consisted of two round inner capillaries inserted inside a square outer capillary. The orifice sizes of the injection and collection capillary were 50 and 430 µm, respectively. The droplet



shells were polymerised by exposure to UV-A radiation with an irradiance of 0.7-38.1 mW·cm<sup>-2</sup> after droplet generation. The inner phase was 5-30 wt% aqueous solution of K<sub>2</sub>CO<sub>3</sub> containing small amounts of the pH indicator m-cresol purple. The middle phase was a UV-curable liquid silicon rubber (Semicosil<sup>®</sup> 949) containing 0-2 wt% Dow Corning 749 Fluid added to stabilise the inner liquid-liquid interface. The outer phase was 60-70 wt% aqueous solution of glycerol containing 0-2 wt% PVA, Tween 20 or Pluronic<sup>®</sup> F-127 added to stabilise the outer interface. The capsules were cut using a microtome and the images of cross-sectioned capsules were taken using a Scanning Electron Microscope (SEM) (Fig. 1c.3).

## Results and discussion

The capsule diameter and the shell thickness were precisely adjusted over the range of 200-400 and 20-30 µm, respectively by controlling the flow rate of the three fluid streams in the microfluidic device. By increasing the outer phase flow rate from 5 to 35 mL/h at the constant inner and middle phase flow rates of 1.5 mL/h, a reduction in the droplet size from 324 to 228 µm was achieved, while the shell thickness remained unchanged at 30 µm. The same behaviour was predicted numerically by Nabavi *et al.* [5]. The coefficient of variation of droplet diameters was less than 2.6%. An increase in the concentration of K<sub>2</sub>CO<sub>3</sub> in the core solution from 5 to 30 wt% at the outer phase flow rate of 5-10 mL/h caused a slight increase in the droplet diameter which could be attributed to the corresponding increase in the viscosity of the compound jet formed in the collection capillary and its higher resistance to pinch off. For inner phase containing 5-15 wt% K<sub>2</sub>CO<sub>3</sub> solution, the presence of 0.5-2 wt% PVA (poly(vinyl alcohol)), 0.5-2 wt% Tween 20, or 0.5-1 wt% Pluronic F127 in the outer phase provided a good drop formation stability. However, In the case of 30 wt% K<sub>2</sub>CO<sub>3</sub> solution in the core, only 0.5 wt% Pluronic F127 could provide a successful long-term drop formation stability.

The minimum UV light irradiance and energy density of 13.8 mW·cm<sup>-2</sup> and 2 J·cm<sup>-2</sup> respectively, corresponding to the minimum exposure time of 144 s were required to achieve a complete shell polymerisation. The core-shell drops made without any lipophilic stabiliser (Dow Corning 749 Fluid) were unstable and released the inner droplet before they had time to polymerise. Adding at least 0.5 wt% Dow Corning 749 Fluid in the organic phase was essential to stabilise the core/shell structure prior to polymerisation. The shells containing 0.5 wt% Dow Corning 749 Fluid were fully solidified ~30 min after UV exposure. However, for 2 wt% Dow Corning 749 Fluid in the shell, the curing time was more than one hour which was attributed to accumulation of the stabiliser at the outer interface of the shell and the reduction in intensity of the incident UV light. When placed in hypotonic solutions, the capsules became swollen due to diffusion of water to the interior of the capsules. For the capsules containing initially 30 wt% K<sub>2</sub>CO<sub>3</sub>, a particle diameter became 4 times

larger than the initial diameter, when they were stored in pure water until the osmotic equilibrium was established. An analytical model was developed to estimate the size of the core,  $D_{1,eq}$ , at equilibrium:

$$(KC_{out})^4 + (1 - KC_{in}) - 1 = 0 \quad (1)$$

where  $s = D_{1,eq}/D_1$ ,  $C_{out}$  and  $C_{in}$  are the equilibrium expansion ratio of the core, and the molarity of storage and core solutions before equilibrium, respectively,  $D_1$  is the initial diameter of the core and  $K$  is

$$K = D_1 RT_i / 8tE \quad (2)$$

where  $R$  is the gas constant,  $T$  is the temperature,  $i$  is the van 't Hoff factor,  $E$  is the elastic modulus, and  $t$  is the initial shell thickness.

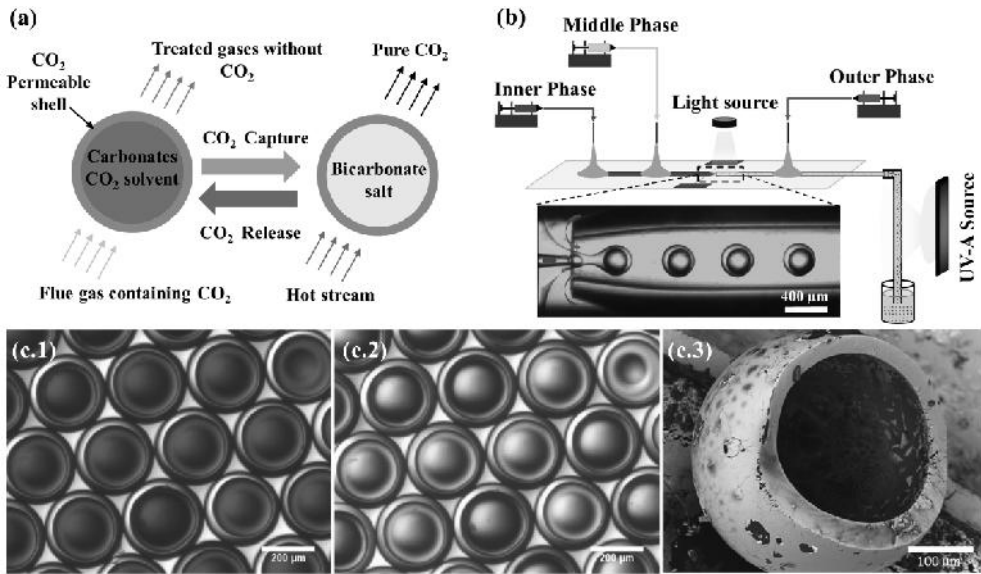


**Fig. 1.** (a) A principle of CO<sub>2</sub> capture and release using fabricated capsules; (b) The experimental set-up consisting of a glass capillary device for droplet generation, syringe pumps for delivery of the liquids to the device, an inverted microscope for observation of drop generation and a UV-A source for on-the-fly *in-situ* photo-polymerisation of the shells; (c.1) The synthesised capsules prior to CO<sub>2</sub> capture test (pH > 11), scale bar = 200 μm. (c.2) Capsules after CO<sub>2</sub> capture (pH < 8), scale bar = 200 μm. (c.3) SEM image of a microtome cross-sectioned capsule, scale bar = 100 μm.

Prior to CO<sub>2</sub> uptake, the capsule interiors were purple because the pH was above 11 (**Fig. 1c.1**). After exposure to CO<sub>2</sub>, the colour of the core liquid turned yellow (**Fig. 1c.2**), due to decrease in pH below 8 caused by the chemical reaction:  $\text{K}_2\text{CO}_3 + \text{H}_2\text{O} + \text{CO}_2 \rightarrow 2\text{KHCO}_3$ . The capsule can be regenerated by heating, which can cause the reaction to proceed in the opposite direction and a pure stream of CO<sub>2</sub> is released:  $2\text{KHCO}_3 \rightarrow \text{CO}_2 + \text{K}_2\text{CO}_3 + \text{H}_2\text{O}$ . Based on the stoichiometry of the CO<sub>2</sub> uptake by potassium carbonate solution, the equilibrium capture capacity of 30 wt% K<sub>2</sub>CO<sub>3</sub> solution is 2.17 mmol/g.

However, due to the volume of the shell, a correction factor of  $\frac{\rho_c D_1}{\rho_s t + \rho_c D_1}$

should be taken into the account, where  $\rho_c$  is the density of core liquid, and  $\rho_s$  is the density of cured shell. Therefore, the actual CO<sub>2</sub> capture capacity of 30 wt% K<sub>2</sub>CO<sub>3</sub> capsules was 1.6-2 mmol/g and the exact value was dependant on the size and shell thickness of the capsules. The capsules were thermally stable up to 450°C, as confirmed by thermogravimetric analysis (TGA). The drop fabrication process was stable over a period of at least one hour with a maximum deviation of droplet sizes of 4.3%.

## Conclusions

A novel process for the production of highly uniform elastic capsules filled with aqueous K<sub>2</sub>CO<sub>3</sub> solutions was developed consisting of generation of core/shell drops in a microfluidic device and “on-the-fly” photopolymerisation of the shell initiated by UV irradiation. The size of the capsules and their shell thickness were precisely tuned by controlling the flow rate of the three fluid streams in the microfluidic device. The minimum UV light irradiance, energy density and exposure time for a complete shell polymerisation were 13.8 mW·cm<sup>-2</sup>, 2 J·cm<sup>-2</sup>, and 144 s, respectively. An analytical model was developed to estimate the morphological changes of the capsules during storage caused by the osmotic stress. The optimum hydrophobic stabilizer for continuous production of capsules with 30 wt% K<sub>2</sub>CO<sub>3</sub> in the core was 0.5 wt% Pluronic® F-127. The capture of CO<sub>2</sub> by the capsules was visualised using a dye indicator, m-cresol purple. The CO<sub>2</sub> storage capacity of the capsules containing 30 wt% K<sub>2</sub>CO<sub>3</sub> in the core was found to be 1.6-2 mmol/g based on their size and shell thickness. The shell has a high thermal stability with the onset temperature of degradation at around 450°C, implying that the microcapsules are suitable for high temperature applications.

## Acknowledgment

The authors gratefully acknowledge the financial support for this work from the EPSRC grant EP/H029923/1. The authors also thank Mr Shaun Fowler, Mr Ekanem E. Ekanem, and Dr Konstantin Luponov for their support during the entire experimental work.

## References

- [1] N. MacDowell, N. Florin, A. Buchard, J. Hallett, A. Galindo, G. Jackson, *et al.*, *Energy Environ. Sci.*, 2010, **3**, 1645–1669.
- [2] M.E. Boot-Handford, J.C. Abanades, E.J. Anthony, M.J. Blunt, S. Brandani, N. MacDowell, *et al.*, *Energy Environ. Sci.*, 2014, **7**, 130–189.
- [3] J.J. Vericella, S.E. Baker, J.K. Stolaroff, E.B. Duoss, J.O. Hardin, J. Lewicki, *et al.*, *Nat. Commun.* 2015, **6**, 6124–6130.
- [4] G.T. Vladislavljević, H.C. Shum, D. a. Weitz, *Prog. Colloid Polym. Sci.*, 2012, **139**, 115–118.
- [5] S.A. Nabavi, G.T. Vladislavljević, S. Gu, E.E. Ekanem, *Chem. Eng. Sci.*, 2015, **130**, 183–196.

***Hydrogen storage, batteries and  
electrochemical capacitors***

---



## BOROHYDRIDES AS HYDROGEN STORAGE MATERIALS: MOLECULAR DYNAMICS STUDIES

Anton Gradišek

*Department of Solid State Physics, Jožef Stefan Institute, Jamova 39,  
SI-1000 Ljubljana, Slovenia ([anton.gradisek@ijs.si](mailto:anton.gradisek@ijs.si))*

Complex hydrides are promising materials for solid-state hydrogen storage applications. Hydrogen is covalently bound to atoms of light elements such as Li, Al, B, and Na. Borohydrides have drawn especially high scientific interest due to the high weight percent of stored hydrogen – for example,  $\text{LiBH}_4$  contains almost 20 wt. % of hydrogen. The issue, however, is the hydrogen release, which takes place at high temperatures, due to the covalent nature of bound hydrogen. To overcome this obstacle, various approaches have been attempted to synthesize materials with lower decomposition temperatures, which would make them viable for on-board applications in vehicles. They include introduction of additional elements in the structure, incorporation into nanoporous frameworks, or mixtures with catalysts.

Understanding molecular dynamic processes in these materials is important in view of designing novel systems. NMR is a powerful tool to study dynamics. Dynamic processes can be tracked using various approaches, such as direct diffusion measurements, NMR spectra, and nuclear spin-lattice relaxation time.

I will present an overview of the recent work on some novel borohydride systems, including  $\text{LiZn}_2(\text{BH}_4)_5$  system which consists of a complex network of  $\text{BH}_4$  tetrahedra,  $\text{Sr}(\text{BH}_4)_2(\text{NH}_3)_2$ , where hydrogen is also bound to nitrogen atoms, and  $(\text{NH}_4)_2\text{B}_{10}\text{H}_{10}$  and  $(\text{NH}_4)_2\text{B}_{12}\text{H}_{12}$  systems, where hydrogen is bound to large, almost spherical units. Typical dynamic processes in these systems are rotations/reorientations of hydrogen-containing units around various symmetry axis, for which activation energies can be determined.

# INFLUENCE OF MILLING TIME ON HYDROGEN DESORPTION PROPERTIES OF $\text{LiAlH}_4 - \text{Fe}_2\text{O}_3$ COMPOSITE

I. Milanovic<sup>\*</sup>, S. Milosevic, S. Kurko, M. Savic, R. Vujasin, A. Djukic,  
J. Grbovic Novakovic

*Vinca Institute of Nuclear Sciences, University of Belgrade, Belgrade, Serbia,  
(\*igorm@vinca.rs)*

Complex hydrides, with composition of  $\text{ABH}_x$  (A – light metal, B – transition metal, X – number of hydrogen atoms) are prominent candidates for hydrogen storage applications.  $\text{LiAlH}_4$  which posses 7.9 wt.% of hydrogen and release hydrogen in two step reactions taking place between 150–175°C and 180–220°C. It has been noticed that modification of  $\text{LiAlH}_4$  structure [1], with addition of oxides, give rise to enhancement in hydrogen desorption properties [2]. In that sense composites of  $\text{LiAlH}_4$  with addition of 5 wt.%  $\text{Fe}_2\text{O}_3$  were synthesized by mechanochemical method using different milling times between 0 and 15 minutes. The DSC measurements show that sample milled for 3 minutes exhibit only one desorption peak, while in other samples two desorption maxima has been observed (**Fig. 1**). Desorption properties measured with TPD and DSC were correlated to the microstructural changes of the material caused by mechanical milling. The microstructure was evaluated by: XRD, PSD and FTIR analysis.

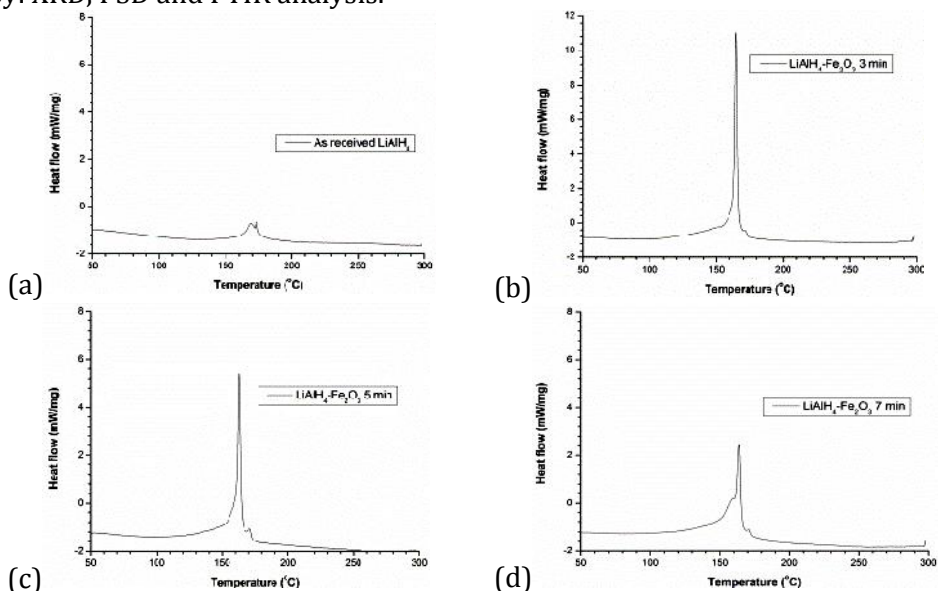


**Fig. 1.** The DSC measurements for pure  $\text{LiAlH}_4$  (a) and milled  $\text{LiAlH}_4\text{-Fe}_2\text{O}_3$  samples: 3(b), 5(c) and 7 min(d).



## References

- [1] Z. Li, P. Li, Q. Wan, J. Phys. Chem. C, 2013, **117**, 18343-18352.
- [2] M. Ismail, A. Sinin, C. Sheng, Int.J. Electrochem. Sci., 2014, **9**, 4959-4973.

# DFT STUDY OF HYDROGEN DESORPTION PROPERTIES OF BORON DOPED $\text{MgH}_2$

Sandra Kurko\*, Radojka Vujasin, Bojana Paskaš Mamula,  
Jasmina Grbović Novaković, Nikola Novaković

*Vinča Institute for Nuclear Sciences, University of Belgrade, P.O. Box 522, 11000  
Belgrade, Serbia (\*[skumric@vinca.rs](mailto:skumric@vinca.rs))*

The goal of this research was to investigate by means of DFT the effects boron introduction in  $\text{MgH}_2$  host matrix has on the hydride structure and its dehydrogenation reaction. The bulk calculations of different structures with various concentrations of boron added showed that if 6.25 at.% of Mg was substituted with B, a formation of stable compound with chemical formula  $\text{Mg}_{15}\text{BH}_{32}$  was possible. Electrical conductivity of doped systems depends on boron concentration, changing from insulating through semiconducting to conducting with the increase of boron quantity. Bader analysis on  $\text{Mg}_{15}\text{BH}_{32}$  compound showed that ionic Mg-H interaction was replaced with stronger covalent B-H bond. NEB calculations showed that introduction of boron leads to decrease of activation energy for neutral hydrogen vacancy diffusion (**Fig. 1**).

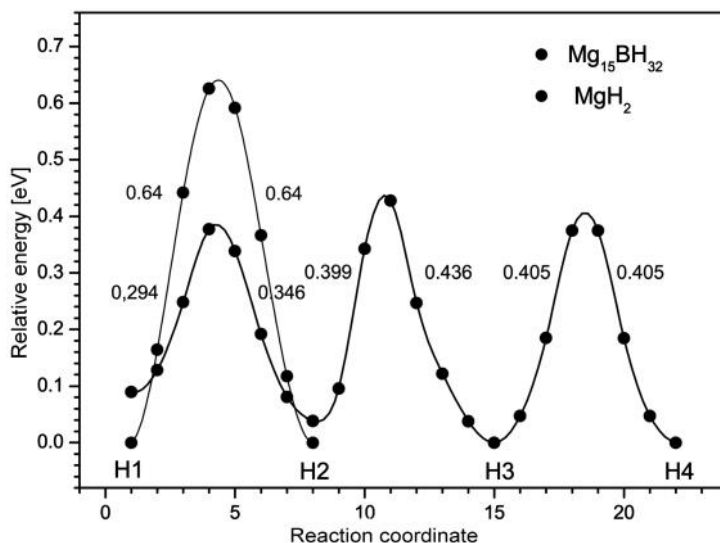


**Fig. 1.** The barrier for hydrogen vacancy diffusion in  $\text{MgH}_2$  and  $\text{Mg}_{15}\text{BH}_{32}$  (four non-equivalent positions).

Slab calculations of (110)  $\text{MgH}_2$  surface with boron embedded in the surface layer showed that hydrogen vacancy formation energy is lower in the boron doped system and decline with increasing distance from boron. Surface hydrogen desorption energy depends on its saturation but also on arrangement of desorbed atoms. In non-doped hydride this energy is the largest for fully occupied surface, while in doped system this energy is significantly smaller. In both systems, desorption energy for incompletely occupied surface strongly depends on desorbed atoms configuration and have irregular trend. Activation energy for hydrogen molecule desorption from (110)  $\text{MgH}_2$  surface depends on desorbed atom configuration and in doped system is slightly smaller than in non-doped if desorbed atoms are further away from introduced boron atom.

## THE PHYSICOCHEMICAL PROPERTIES OF GRAPHENE OXIDE – PHOSPHOTUNGSTIC ACID HYBRID CAPACITOR

Z. Jovanović<sup>1</sup>, D. Bajuk-Bogdanović<sup>2</sup>, M. Vujković<sup>2</sup>, S. Jovanović<sup>1</sup>,  
I. Holclajtner-Antunović<sup>2</sup>

<sup>1</sup>*Laboratory of Physics, Vinča Institute of Nuclear Sciences, University of Belgrade, P.O. Box 522, 11001 Belgrade, Serbia;* <sup>2</sup>*Faculty of Physical Chemistry, University of Belgrade, P.O. Box 47, 11158 Belgrade, Serbia*

In recent years, there is a strong development of novel carbon-based energy storage systems. Among them, graphene oxide (GO), thanks to its high specific surface area, is an ideal platform for integration with different functional materials. In this work, we have investigated the physicochemical properties of hybrid capacitor prepared by combining GO and phosphotungstic acid (WPA). The obtained material has been heat treated in inert atmosphere and characterized by Fourier transform infrared spectroscopy (FTIR), Raman spectroscopy, X-ray photoelectron spectrometry (XPS), temperature programmed desorption (TPD) and cyclic voltammetry. The multipoint Raman mapping confirmed the homogeneity of the samples, whereas the FTIR analysis showed thermal activation of structural changes of WPA. In the case of GO, the FTIR, XPS and TPD analysis showed desorption of oxygen-containing functional groups with temperature increase. The electrochemical properties of the GO/WPA composite were improved in comparison to pristine GO. In our study the highest increase of both capacitance and operating voltage was achieved at 500 °C. The results suggest that optimization of annealing temperature and GO/WPA ratio is an effective pathway for preparation of hybrid supercapacitors with enhanced properties.

# FARADAIC VERSUS PSEUDOCAPACITANCE MECHANISM OF CHARGE STORAGE IN $\text{NaFe}_{0.95}\text{V}_{0.05}\text{PO}_4/\text{C}$ COMPOSITE

Milica Vujković<sup>1,2</sup>, Slavko Mentus<sup>1,2</sup>

<sup>1</sup>*Faculty of Physical Chemistry, University of Belgrade, Studentski trg 12-16, P.O. Box 137, Belgrade, Serbia;* <sup>2</sup>*The Serbian Academy of Science and Arts, Knez Mihajlova 35, 11158 Belgrade, Serbia*

## Abstract

Olivine  $\text{NaFe}_{0.95}\text{V}_{0.05}\text{PO}_4$  in a form of  $\text{NaFe}_{0.95}\text{V}_{0.05}\text{PO}_4/\text{C}$  composite was obtained from  $\text{LiFe}_{0.95}\text{V}_{0.05}\text{PO}_4/\text{C}$  composite by electrochemical ion replacement in aqueous  $\text{NaNO}_3$  solution, which was carried out by cyclic voltammetry. The coulombic capacity of  $\text{NaFe}_{0.95}\text{V}_{0.05}\text{PO}_4$  in  $\text{NaNO}_3$  solution was measured galvanostatically to amount to  $\sim 105 \text{ mAh g}^{-1}$  and  $\sim 85 \text{ mAh g}^{-1}$  at current densities of  $154 \text{ mA g}^{-1}$  and  $5000 \text{ mA g}^{-1}$ , respectively, which is significantly better compared to that of  $\text{LiFe}_{0.95}\text{V}_{0.05}\text{PO}_4$  in  $\text{LiNO}_3$  solution. Capacity increase is primarily due to the pseudocapacitance kind of charge storage rise during the sodiation/desodiation process.

## Introduction

An increasing demand for both high-energy and high-power metal-ion rechargeable batteries caused the interest of researchers for pseudocapacitive intercalate materials which are promising in this sense. These materials, usually nanoparticulate in nature, can provide very fast charging/discharging reactions, taking place at or near the electrode surface and having pseudocapacitor-like behavior [1,2]. In this paper, the sodiation of lithiated olivine  $\text{LiFe}_{0.95}\text{V}_{0.05}\text{PO}_4$  was found to shift the charge storage mechanism toward the pseudocapacitance one. Because of that, the composite  $\text{NaFe}_{0.95}\text{V}_{0.05}\text{PO}_4/\text{C}$  exhibits both higher charge storage capacity and faster intercalation/deintercalation reactions compared to its lithium counterpart.

## Experimental

$\text{NaFe}_{0.95}\text{V}_{0.05}\text{PO}_4/\text{C}$  composite, which may not be directly synthesized, was obtained by potentiodynamic cycling of  $\text{LiFe}_{0.95}\text{V}_{0.05}\text{PO}_4/\text{C}$  in an aqueous solution of  $\text{NaNO}_3$ , as described in ref. [3,4]. Such obtained electrode was subjected to further examination in  $\text{NaNO}_3$  by both cyclic voltammetry (CV) and chronopotenciometry (CP). For the sake of comparison,  $\text{LiFe}_{0.95}\text{V}_{0.05}\text{PO}_4/\text{C}$  was examined in an aqueous  $\text{LiNO}_3$  solution. CV and CP measurements were performed in a three-electrode cell, with Pt counter electrode, and saturated calomel electrode (SCE) as reference one, connected to a Gamry PCI4/300 Potentiostat/Galvanostat measuring device.

## Results and discussion

CVs of  $\text{NaFe}_{0.95}\text{V}_{0.05}\text{PO}_4/\text{C}$  and its lithiated precursor, measured in  $\text{NaNO}_3$  and  $\text{LiNO}_3$ , are shown in **Fig.1**. CV of  $\text{MFe}_{0.95}\text{V}_{0.05}\text{PO}_4/\text{C}$  ( $\text{M}=\text{Na}$  or  $\text{Li}$ ), as the finger print, clearly shows the differences between redox behavior of lithiated and sodiated olivine. The  $\text{LiFe}_{0.95}\text{V}_{0.05}\text{PO}_4 \rightarrow \text{Fe}_{0.95}\text{V}_{0.05}\text{PO}_4$  phase transition occurs directly, as evidenced by the appearance of one pair redox peaks. The  $\text{NaFe}_{0.95}\text{V}_{0.05}\text{PO}_4 \rightarrow \text{Fe}_{0.95}\text{V}_{0.05}\text{PO}_4$  phase transition happens via formation of the intermediate  $\text{Na}_{0.7}\text{Fe}_{0.95}\text{V}_{0.05}\text{PO}_4$  phase [5], which is visible as anodic peak splitting.

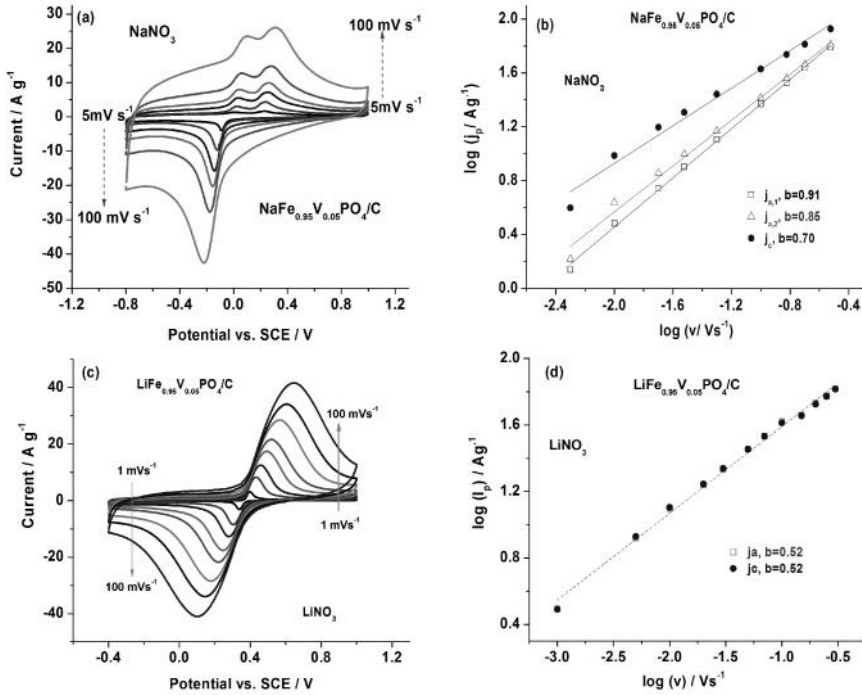


**Fig. 1.** CVs (a,c) and corresponding  $\log I_p$ - $\log v$  dependence (b,d) for  $\text{MFe}_{0.95}\text{V}_{0.05}\text{PO}_4/\text{C}$  ( $\text{M}=\text{Na}$  and  $\text{Li}$ ) measured in aqueous  $\text{NaNO}_3$  and  $\text{LiNO}_3$  at various scan rates, respectively.

By using the  $\log I_p$ - $\log v$  dependence (**Fig.1b, d**), derived from corresponding redox peaks, the exponent  $b$  of the equation  $I=av^b$  was determined. For lithiation/delithiation reactions we found  $b \sim 0.5$ , indicating a preferably bulk faradaic behavior of  $\text{LiFe}_{0.95}\text{V}_{0.05}\text{PO}_4/\text{C}$ , which is in agreement with the literature [1]. The  $b$ -values for sodiation/desodiation reactions were found to amount to 0.7 (cathodic peak), 0.85 (1<sup>st</sup> anodic peak) and 0.91 (2<sup>nd</sup> anodic peak), which indicates the dominance of surface charge-transfer processes. It

can be concluded that higher fraction of surface against bulk storage sites was found for sodium than for lithium olivine form. Accordingly, at high charge/discharge rates, the  $\text{NaFe}_{0.95}\text{V}_{0.05}\text{PO}_4/\text{C}$  exhibits enhanced specific capacity compared to  $\text{LiFe}_{0.95}\text{V}_{0.05}\text{PO}_4/\text{C}$ , as shown in **Fig. 2**.

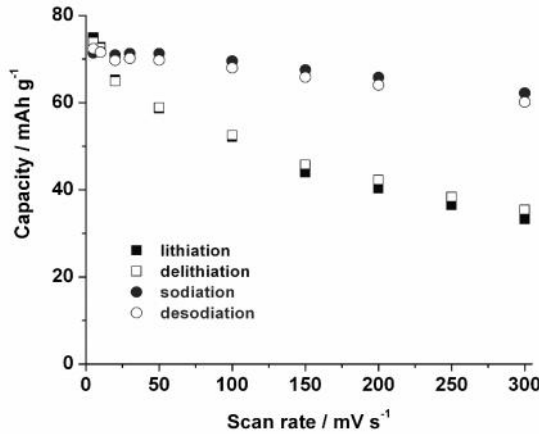


**Fig. 2.** Specific capacity of  $\text{MFe}_{0.95}\text{V}_{0.05}\text{PO}_4/\text{C}$  ( $\text{M} = \text{Na}$  and  $\text{Li}$ ) in  $\text{NaNO}_3$  and  $\text{LiNO}_3$  obtained from CVs.

The sodium and lithium charge storage capacities in the olivine are similar at scan rates below  $20 \text{ mV s}^{-1}$ . Namely, when the scan rate is low, metal ions have enough time to penetrate into the depth of the olivine phase, so that the difference in the redistribution of the "inner" and "outer" charge between lithium and sodium storage doesn't affect the value of the measured capacity. However, when the polarization rate is high, preferably the outer surface becomes available for charge storage. So, at high sweep rates, larger capacity of  $\text{NaFe}_{0.95}\text{V}_{0.05}\text{PO}_4/\text{C}$  compared to  $\text{LiFe}_{0.95}\text{V}_{0.05}\text{PO}_4/\text{C}$  was measured, due to the increase of pseudocapacity fraction in overall coulombic capacity.

Galvanostatic CP curves of  $\text{NaFe}_{0.95}\text{V}_{0.05}\text{PO}_4/\text{C}$  in  $\text{NaNO}_3$ , measured at various charging/discharging rates, were shown in **Fig. 3a**. High sodium storage capacities, ranging from  $83\text{-}100 \text{ mAh g}^{-1}$ , were measured in the range from  $54 \text{ mA g}^{-1}$  (1C) to  $5000 \text{ mA g}^{-1}$  ( $\sim 33\text{C}$ ). The appearance of two plateaus during desodiation process, corresponding to a two-phase transition, is in accordance with the CV curves. However, these plateaus are poorly defined due to pseudocapacitance nature of the nanoparticulate  $\text{NaFe}_{0.95}\text{V}_{0.05}\text{PO}_4/\text{C}$  composite [3,4].

The appearance of two plateaus, can be better seen through the first derivative ( $dQ/dV$ ) of CP curve (**Fig. 3**). In that way one can see that the sodiation process also occurs through two steps, analogously to desodiation. According to the shape of  $dQ/V$  curve, it can be concluded that the first phase

transition step,  $\text{Fe}_{0.95}\text{VPO}_4 \rightarrow \text{Na}_{0.7}\text{Fe}_{0.95}\text{PO}_4$ , is controlled by solid-state diffusion (sharp  $dQ/dV$  peak) while the other phase transition step,  $\text{Na}_{0.7}\text{Fe}_{0.95}\text{PO}_4 \rightarrow \text{NaFe}_{0.95}\text{PO}_4$ , as well as both desodiation redox processes are free from the limitations of solid-state diffusion (broad  $dQ/dV$  peaks together with the deviation of baseline from zero). Accordingly, some redistributions of ions happen during the charging/discharging. During sodiation, some parts of  $\text{Na}^+$  ions, assigned as  $\text{Na}_{\text{I}}^+$ , probably occupy bulk positions in the step  $\text{Fe}_{0.95}\text{VPO}_4 \rightarrow \text{Na}_{0.7}\text{Fe}_{0.95}\text{PO}_4$ , while the other part, assigned as  $\text{Na}_{\text{II}}^+$  participating in the step  $\text{Na}_{0.7}\text{Fe}_{0.95}\text{PO}_4 \rightarrow \text{NaFe}_{0.95}\text{PO}_4$ , occupies surface sites. During deintercalation, the  $\text{Na}_{\text{I}}^+$  ions leave the surface sites, while at the same time the  $\text{Na}_{\text{II}}^+$  ions migrate into vacated  $\text{Na}_{\text{I}}^+$  surface sites. Having in mind that the second anodic phase transition ( $\text{Na}_{0.7}\text{Fe}_{0.95}\text{PO}_4 \rightarrow \text{Fe}_{0.95}\text{PO}_4$ ) may take place only after the termination of the first anodic phase transition, both redox processes during anodic scan involve a higher fraction of surface charge and thus show the pseudocapacitance behavior.

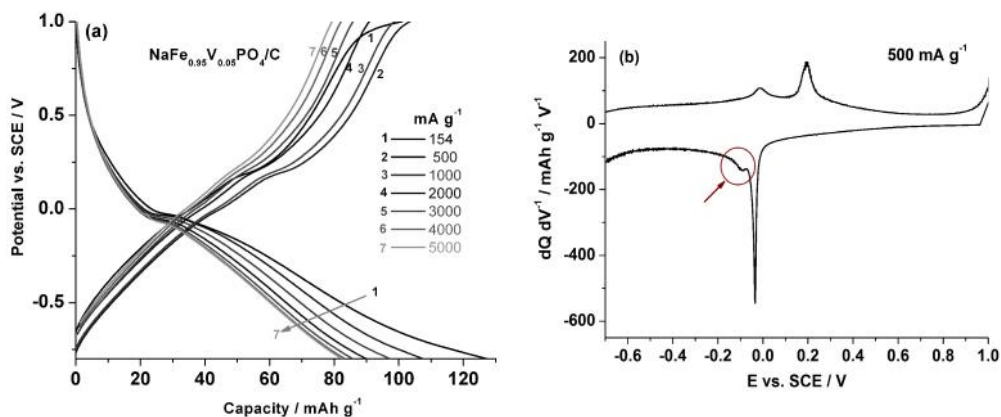


**Fig. 3.** The CP curves of  $\text{NaFe}_{0.95}\text{V}_{0.05}\text{PO}_4/\text{C}$  in  $\text{NaNO}_3$  solution at various charge/discharge rates (a) and the first derivative ( $dQ/dV$ ) of CP curve at rate of  $500 \text{ mA g}^{-1}$  (b).

## Conclusion

The  $\text{NaFe}_{0.95}\text{V}_{0.05}\text{PO}_4/\text{C}$  composite involving olivine  $\text{NaFe}_{0.95}\text{V}_{0.05}\text{PO}_4$  was obtained by electrochemical ion exchange of  $\text{LiFe}_{0.95}\text{V}_{0.05}\text{PO}_4/\text{C}$  composite in aqueous solution of sodium nitrate. While in  $\text{LiFe}_{0.95}\text{V}_{0.05}\text{PO}_4/\text{C}$  charge storage happens through a bulk diffusion-controlled mechanism, in  $\text{NaFe}_{0.95}\text{V}_{0.05}\text{PO}_4/\text{C}$  charge storage mechanism is shifted preferably towards pseudocapacitance one. Thanks to that, the  $\text{NaFe}_{0.95}\text{V}_{0.05}\text{PO}_4/\text{C}$  shows significantly higher capacity than  $\text{LiFe}_{0.95}\text{V}_{0.05}\text{PO}_4/\text{C}$  at scan rates higher than  $30 \text{ mV s}^{-1}$ . Moreover, high sodiation/desodiation capacity of  $\text{NaFe}_{0.95}\text{V}_{0.05}\text{PO}_4/\text{C}$  ( $\sim 105 \text{ mAh g}^{-1}$  @  $154 \text{ mA g}^{-1}$ ) was found, being very promising for high power aqueous rechargeable batteries.



### Acknowledgement

This work was supported by the Ministry of Education, Science and Technological Development of the Serbia Republic through the Project III 45014.

### References

- [1] P. Simon, Y. Gogotsi, B. Dunn, *Science*, 2014, **343**, 1210-1211.
- [2] V. Augustyn, J. Come, M.A. Lowe, J.W. Kim, P.-L. Taberna, S.H. Tolbert, H.D. Abruña, P. Simon, B. Dunn, *Nature Materials*, 2013, **12**, 518-522.
- [3] M. Vujković, D. Jugović, M. Mitrić, I. Stojković, N. Cvjetičanin, S. Mentus, *Electrochim. Acta*, 2013, **109**, 835-842.
- [4] M. Vujković, S. Mentus, *J. Power Sources*, 2014, **247**, 184-188.
- [5] P. Moreau, D. Gyomard, J. Gaubicher, F. Biucher, *Chem. Mater.* 2010, **22**, 4126-4128.

# VO<sub>2</sub> POLYMORPH B AS A ELECTRODE MATERIAL IN ORGANIC AND AQUEOUS Li-ION BATTERIES

Sanja Milošević<sup>1</sup>, Ivana Stojković Simatović<sup>2</sup>, Sandra Kurko<sup>1</sup>,  
Jasmina Grbović Novaković<sup>1</sup>, Nikola Cvjetičanin<sup>2</sup>

<sup>1</sup>*Vinča Institute of Nuclear Sciences, Department of Materials Science, University of Belgrade, Belgrade, Serbia,* <sup>2</sup>*Faculty of Physical Chemistry, University of Belgrade, Belgrade, Serbia*

## Abstract

Requirements for safe and environmental friendly Li-ion batteries with high and stable capacity are increasing each year. Investigation of novel electrode materials and their combination with suitable electrolytes requires a lot of effort and time in order to reach satisfactory performance. It has been demonstrate that solvothermally synthesised VO<sub>2</sub>(B) is a promising electrode material for organic and aqueous Li-ion batteries, with a initial capacity of 119 mAh/g and 177 mAh/g, respectively.

## Introduction

Li-ion batteries are widely used in portable electrical devices and their use in electric vehicles is rapidly gaining momentum. Variety of materials and different electrolytes has been tested for years and today's batteries are considered safe for commercial use. In commercial Li-ion batteries only organic electrolytes are in use, while aqueous-electrolyte batteries are neglected and still remains in the field of scientific experiments. Limited voltage of 1.5V, small values of capacity as well as capacity retention in aqueous electrolyte are main constraints for commercial usage. Yet, VO<sub>2</sub>(B) proved to be promising electrode material in both aqueous [1] and organic Li-ion batteries with exceptional capacity and excellent stability. Solvothermal synthesis of VO<sub>2</sub>(B) results in a mixture of particles with a different morphology and size, which appeared to be suitable for stable electrochemical performances. VO<sub>2</sub>(B) is a semiconductor [1] which is very important for electrode material, but morphology of particles play important role also [2].

## Results and discussion

VO<sub>2</sub>(B) was synthesized using a one-step solvothermal method [3] and confirmed by X-ray diffraction. A mixture of micro and nano-sized particles was observed using SEM analysis and this robust microstructure is the most probable reason for excellent electrochemical activity and constant capacity. X-ray diffraction results of obtained black-bluish powder, represented in **Fig. 1**, confirmed a successfully synthesized VO<sub>2</sub> polymorph type B. Diffraction pattern

of monoclinic  $\text{VO}_2(\text{B})$  corresponds to JCPDS Card No. 31-1438 or ICSD 73855. The X-ray powder diffraction measurements were performed by Siemens Kristallflex D-500 diffractometer using  $\text{Cu K}\alpha_{1,2}$  radiation in  $2\theta^\circ$  range from 10 to  $75^\circ$  using  $0.02^\circ$  step and exposition time of 5 s.

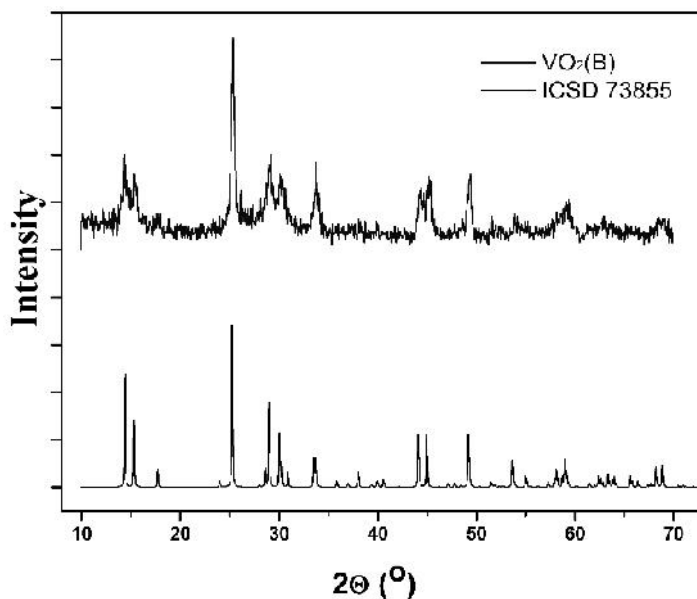


**Fig. 1.** XRD pattern of  $\text{VO}_2(\text{B})$  powder material obtained by solvothermal synthesis (blue) and corresponding  $\text{VO}_2(\text{B})$  pattern ICSD 73855 (black).

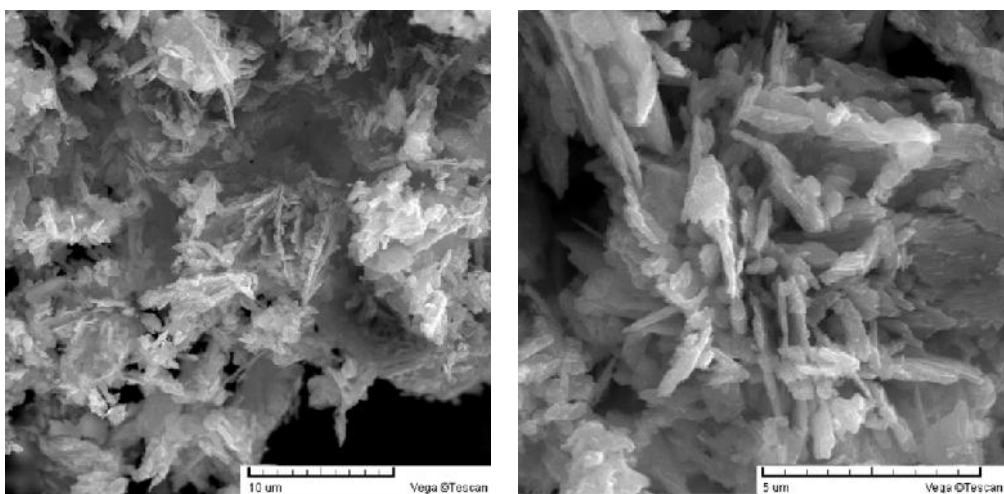


**Fig. 2.** SEM micrographs of obtained  $\text{VO}_2(\text{B})$ ; left marker 10µm, right marker 5µm.

Morphological characterization was carried out by SEM VEGA TS 5130MM, Tescan Brno. Obtained micrographs are presented in **Fig. 2**.  $\text{VO}_2(\text{B})$  powder consists of single nanoparticles, rods and flat particles, mutually welded in different irregularly shaped micrometer-sized structures. Observed particles very much look like particles observed in process of Ostwald ripening but without the last step in flower formation [2].

Galvanostatic charge/discharge experiments were carried out at room temperature using software-controlled Arbin BT-2042 instrument. The two-electrode arrangement was used for these measurements, with  $\text{VO}_2(\text{B})$  as the active material of the working electrode, and lithium metal foil as a counter electrode, in organic electrolyte solution (1M  $\text{LiClO}_4$  in propylene carbonate). The constant current cycling performances of synthesized cathode material have been tested within the voltage range of 3.2–2.0V, at current density of 50mA/g. The charging/discharging curves of  $\text{VO}_2(\text{B})$  cathode are shown in **Fig. 3**, and discharge plateau at  $\sim 2.6\text{V}$  is notable. Values of discharge capacity during these 50 cycles are presented in **Fig. 4**.

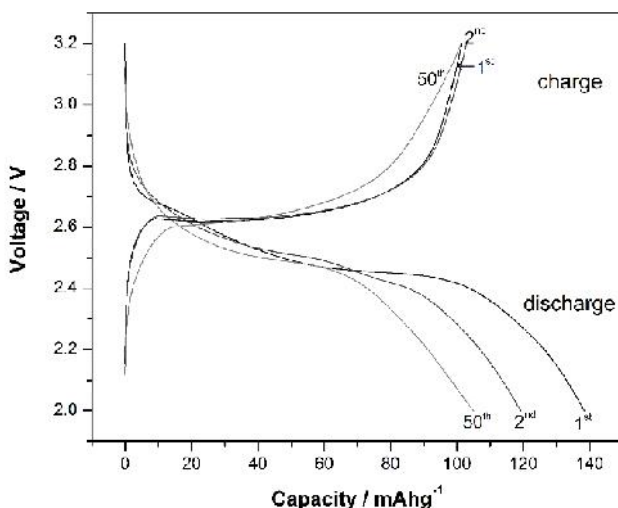


**Fig. 3.** Charge–discharge curves for 1<sup>st</sup>, 2<sup>nd</sup> and 50<sup>th</sup> cycle. The current rate is 50mA/g.

The discharge capacity of the first cycle was 138 mAh/g and of the second 119 mAh/g, which corresponds to irreversible capacity loss in organic electrolyte solutions, attributed to the formation of protective solid electrolyte film on the surface of electrode material [4]. The discharge capacity became more stable in the following cycles and in the 50<sup>th</sup> cycle amounted to 105 mAh/g. The capacity fade between 2<sup>nd</sup> and 50<sup>th</sup> cycle was less than 12%. Capacity fade between 30<sup>th</sup> and 50<sup>th</sup> cycle is negligible.

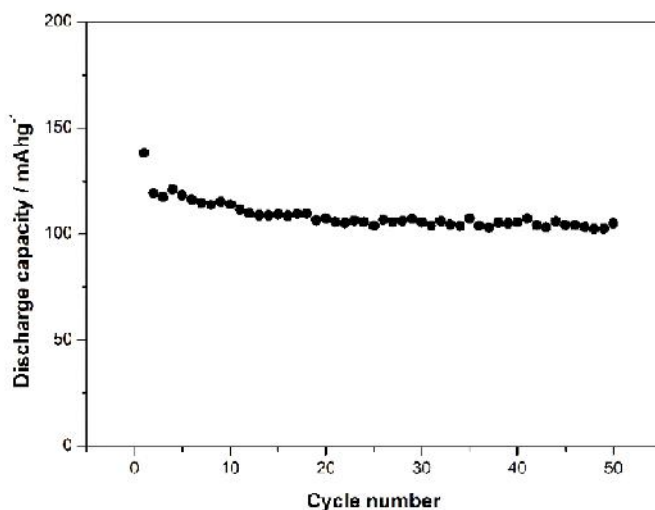


**Fig. 4.** Discharge capacity of VO<sub>2</sub>(B) cathode in an organic electrolyte solution over 50 cycles, at a current rate of 50 mA/g.

VO<sub>2</sub>(B) was also tested in aqueous electrolyte [1] and showed great results (capacity of 170 mAh/g) even at higher current densities with negligible capacity fade (only 4%). Possible reasons for these excellent performances could be: VO<sub>2</sub>(B) microstructure which is robust enough when exposed to an aqueous electrolyte, resulting in a stable intercalation capacity of lithium ions, as well as good electronic conductivity of VO<sub>2</sub>(B) and extremely small charge transfer resistance (1.8 Ω,) [1] providing fast transport of electrons.

## Conclusion

VO<sub>2</sub>(B) obtained by simple, solvothermal synthesis can be used either as cathode material in organic Li-ion batteries, or as anode material in aqueous Li-ion batteries. This superior electrode material provides great capacity and excellent capacity retention.

## References

- [1] S. Milošević, I. Stojković, M. Mitrić, N. Cvjetićanin, J. Serb. Chem. Soc. 2015, **80**(5), 685–694.
- [2] S. Zhang, Y. Li, Ch. Wu, F. Zheng, Y. Xie, J. Phys. Chem. 2009, **C113**, 15058–15067.
- [3] S. Milošević, I. Stojković, S. Kurko, J. Grbović Novaković, N. Cvjetićanin, Ceram. Int. 2012, **38**(3), 2313–2317.
- [4] I. Stojković, N. Cvjetićanin, S. Mentus, Electrochem. Commun. 2010, **12**, 371–373.



***Theory***

---





# ELECTRONIC STRUCTURE INVESTIGATION OF $\text{AlH}_3$ POLYMORPHS

Milijana Savić, Jana Radaković, Katarina Batalović

*Vinča Institute of Nuclear Sciences, University of Belgrade, P.O. Box 522, 11001  
Belgrade, Serbia*

$\text{AlH}_3$  polymorphs ( $\alpha$ -,  $\beta$ -,  $\gamma$ -) are investigated using theoretical approach DFT (density functional theory) [1]. The study is focused on electronic properties. Unit cells of studied alanes are hexagonal, cubic and orthorhombic for  $\alpha$ -,  $\beta$ - and  $\gamma$ - $\text{AlH}_3$  respectively. Electronic structure calculations are performed using full potential linearized augmented plane waves + local orbital (FP LAPW+lo) as implemented in program package Wien2k [2]. Results obtained using generalized gradient approximation of Perdew–Burke–Ernzerhof (GGA-PBE) [3] for exchange-correlation and modified Becke-Johnson (mBJ) for exchange potential [4] are presented. Bader’s quantum theory of atoms in molecules (AIM) [5] is used to investigate character of bonds. Calculated properties are in agreement with theoretical and experimental investigations reported previously. Enthalpy term, i.e. the stability of Al-H bond is addressed in detail. Formation enthalpies show similar values for  $\alpha$ -,  $\beta$ - and  $\gamma$ -  $\text{AlH}_3$ , while  $\beta$ - $\text{AlH}_3$  is identified as the most stable. Based on interatomic distances and density of states integration, bond strength and hydride stability are discussed. To avoid the DFT’s inability to predict exact band gap, mBJ potential is used. Systematic increase of the calculated band gaps is seen. Obtained band gap for  $\alpha$ -polymorph is in agreement with reported results obtained using  $G_0W_0$  method.  $\beta$ - polymorph shows the greatest gap indicating greater interaction between electrons, while  $\gamma$ - shows delocalized electrons suggesting good electron mobility. According to criterion which includes values of electron density and its Laplacian, it is concluded that studied alanes show predominantly ionic bond character. Laplacian of electron density is the highest in case of  $\beta$ - $\text{AlH}_3$  which also shows the greatest change in calculated Bader’s charge after using mBJ potential.

## References

- [1] W. Kohn, P. Hohenberg, Phys. Rev. 3B, 1964, **136**, 864-871.
- [2] P. Blaha, K. Schwarz, G.K.H. Madsen, D. Kvasnicka, J. Luitz, Wien, Austria, 2001. ISBN 3-9501031-1-2.
- [3] J.P. Perdew, K. Burke, M. Ernzerhof, PRL 18, 1996, **77**, 3865-3868.
- [4] P. Blaha, F. Tran, PRL, 2009, **102**, 226401-226404.
- [5] R.F. W. Bader, J. Phys. Chem. A 37, 1998, **102**, 7314–7323.

## MATERIALS AT HIGH TEMPERATURES: A FIRST-PRINCIPLES THEORY

Sergei I. Simak

*Department of Physics, Chemistry and Biology (IFM), Linköping University, SE-581 83 Linköping, Sweden*

The energy related materials, which are in focus of the present conference, might work at external conditions that involve high temperature. Accordingly, their proper theoretical description should include a treatment of lattice dynamics. We show how the lattice dynamics at high temperatures can be taken into account within the first-principles modeling. The new methodology is based on first-principles molecular dynamics simulations and provides a consistent way to extract the best possible harmonic or higher order potential energy surface at finite temperatures. It is designed to work for systems with high degree of anharmonicity, i.e. in the cases when the traditional quasiharmonic approximation fails. The accuracy and convergence of the method are controlled in a straightforward way. Excellent agreement of the calculated vibrational spectra at finite temperature with experimental results is demonstrated. The ability of the method to predict phase equilibria at high-temperature conditions is also illustrated.

# THERMODYNAMICS AND FORMATION MECHANISM OF $\text{Gd}_{0.5}\text{M}_{0.5}\text{Cu}_5$ ( $\text{M}=\text{Mg}, \text{Ca}$ ) ALLOY FROM FIRST PRINCIPLES

Jana Radaković, Katarina Batabović, Milijana Savić

*Vinča Institute of Nuclear Sciences, University of Belgrade, P.O. Box 522, 11001  
Belgrade, Serbia*

Most rare earth–transition metal–Mg or Ca compounds can be prepared directly from pure elements, however in order to evaluate the potential stability of hypothetical compounds it is essential to initially determine the starting reaction and reactants. First principles calculations allow one to study hypothetical materials or the ones obtained with great difficulty.

In the work of Krnel *et al.* authors showed that the stable intermetallic phase  $\text{Gd}_{0.54}\text{Ca}_{0.42}\text{Cu}_5$  forms between two immiscible elements (Ca and Gd) when a third element (Cu), which composes stable compounds with both elements, is added to the mix. [1]. The structural model of this alloy is addressed in the experiment, thus provided a starting point for the estimation of synthesis mechanism from the theoretical point of view. To establish the combination of reactants that yield a stable alloy, its final stability is determined by calculating the formation enthalpy from three different starting reactions. Gd is also substituted with Mg, as an alternative to Ca, in order to test the stability of hypothetical  $\text{Gd}_{0.5}\text{Mg}_{0.5}\text{Cu}_5$  compound, simulate its potential formation mechanism and compare it with the results for  $\text{Gd}_{0.5}\text{Ca}_{0.5}\text{Cu}_5$ . Calculations are performed using a full-potential linearized augmented plane-wave method, as implemented in Wien2k, a program package based on density functional theory. Obtained results indicated that the starting structures from which the enthalpy is calculated directly affect the stability of the formed compound. Negative formation enthalpy is obtained for all combinations, but alloys are most stable if synthesized from pure elements. To understand the background of this outcome, and the reason for decreased stability when Gd–Cu alloy is mixed with additives Ca and Mg, research included the analysis of thermodynamics of Ca or Mg mixing with imperfect  $\text{Gd}_x\text{Cu}_5$  ( $x = 0.5, 0.75, 0.875$ ).

## References

[1] M. Krnel, S. Vrtnik, P. Kozelj, A. Kocjan, Z. Jagličić, P. Boulet, M. C. de Weerd, J.M. Dubois, J. Dolinsek. *Phys. Rev. B*, 2016, **93**, 094202.

## STRUCTURAL AND ATOMIC CONFIGURATIONAL ASPECTS OF Cu<sub>3</sub>Pt CATALYSTS

A. V. Ruban

*Royal Institute of Technology (KTH), Sweden; Materials Center Leoben (MCL),  
Austria*

Phase equilibria and atomic configuration of the bulk and surface of CuPt alloys are theoretically investigated at different temperatures using atomic scale simulation techniques based on interactions obtained in first-principles calculations as a first step to answer the question why these alloys are so special for oxygen reduction reaction.

## ***Electrocatalysis***

---



# **Pd-MODIFIED X ZEOLITE ELECTRODES FOR HYDROGEN EVOLUTION REACTION IN ALKALINE MEDIUM**

Milica Vasić<sup>1</sup>, Maria Čebela<sup>2</sup>, Radmila Hercigonja<sup>1</sup>, Diogo M. F. Santos<sup>3</sup>,  
Biljana Šljukić<sup>1,3</sup>

<sup>1</sup>*Faculty of Physical Chemistry, University of Belgrade, Studentski trg 12-16, Belgrade, Serbia;* <sup>2</sup>*Institute of Nuclear Sciences "Vinča", University of Belgrade, Mike Petrovića Alasa 12-14, 11001 Belgrade, Serbia;* <sup>3</sup>*CeFEMA, Instituto Superior Técnico, Universidade de Lisboa, 1049-001 Lisbon, Portugal*

Hydrogen energy as a potential replacement for fossil fuels has been attracting great scientific interest in recent time [1,2]. Advantages of this kind of energy source include high energy content and no greenhouse gas emissions. A simple and environmentally friendly way to produce hydrogen is water electrolysis. Pd belongs to the Pt-group metals and exhibit relatively high electrocatalytic activity for the water electrolysis [3], while its price is lower than that of Pt. Zeolites represent aluminosilicate minerals with high specific surface area and nano-sized cavities, and can be interesting as supporting materials for metal catalysts [4-6].

Herein, Pd-modified X zeolite was prepared by ion exchange from Pd acetate solution and subsequently, electrodes based on the prepared material without and with the addition of activated carbon ("X" and "XC", respectively) were fabricated. The electrodes were tested for hydrogen evolution reaction (HER) in alkaline medium (8 M KOH) using linear scan voltammetry and electrochemical impedance measurements. The reaction parameters including Tafel slope and exchange current density were determined for both electrodes. Similar performance for HER was observed for the examined electrodes, with lower charge transfer resistance in the case of the XC.

## **Acknowledgements**

The authors would like to thank to the Ministry of Education, Science and Technological Development of Republic of Serbia for support within the projects Nos. OI172043, OI172018, 172057 and III45012, as well as to Fundação para a Ciência e a Tecnologia (FCT, Portugal) for postdoctoral research grant no. SFRH/BPD/77768/2011 (B. Šljukić) and for contract no. IF/01084/2014/CP1214/CT0003 under IF2014 Programme (D.M.F. Santos).

## **References**

- [1] J.A. Turner, *Science*, 2004, **305**, 972-974.
- [2] M.T.M. Koper, E. Bouwman, *Angew. Chem. Int. Ed.*, 2010, **49**, 3723-3725.
- [3] L. Zhang, Q. Chang, H. Chen, M. Shao, *Nano Energy*, doi: 10.1016/j.nanoen.2016.02.044.

- [4] Z. Mojović, S. Mentus, Z. Tešić, Mater. Sci. Forum, 2004, **453-454**, 257-262.
- [5] A.A. El-Shafei, A.M. Abd Elhafeez, H.A. Mostafa, J. Solid State Electrochem., 2010, **14**, 185-190.
- [6] Z. Mojović, T. Mudrinić, P. Banković, N. Jović-Jovičić, A. Ivanović-Šašić, A. Milutinović-Nikolić, D. Jovanović, J. Solid State Electrochem., 2015, **19**, 1993-2000.



# **SIMULTANEOUS ELECTROCHEMICAL REDUCTION OF GRAPHENE OXIDE AND DEPOSITION OF NICKEL: EFFECT OF REDUCTION TIME ON CATALYTIC PROPERTIES TOWARDS THE HYDROGEN EVOLUTION REACTION**

Sanjin Gutić<sup>1</sup>, Ana S. Dobrota<sup>2</sup>, Igor A. Pašti<sup>2</sup>

<sup>1</sup>*Department of Chemistry, Faculty of Science, Zmaja od Bosne 33-35, 71000 Sarajevo, Bosnia and Herzegovina;* <sup>2</sup>*University of Belgrade, Faculty of Physical Chemistry, Studentski trg 12-16, 11158 Belgrade, Serbia*

## **Abstract**

Voltammetric behaviour for the hydrogen evolution reaction in alkaline medium was investigated on reduced graphene oxide-nickel composites prepared by simultaneous electrochemical reduction of graphene oxide film and deposition of nickel. Time of reduction was varied in order to obtain surfaces with different Ni/rGO ratios. Obtained results indicate significant promotion effect of reduced graphene oxide on the electrocatalytic performance of nickel and its 'vulcanic' dependence on the reduction (deposition) time.

## **Introduction**

Hydrogen oxidation reaction (HOR) and hydrogen evolution reaction (HER) are essential reactions in hydrogen-based energy technologies[1]. Development of modern alkaline fuel cells and systems for production of hydrogen gas of high purity leads to development of systems based on alkaline electrolyte. Major drawback of these alkaline-based systems is fact that sufficient rates for practical applications can be achieved with expensive precious metal-based catalysts[1,2]. Considering their price and availability, quest for the cheaper and environmentally friendly materials with satisfactory electrocatalytic properties is one of the major tasks in this field.

Promoting effects of carbon on catalytic properties of metals are well known and are achieved through the spillover effect[3,4] which, in case of HER, provides low activation energy path for recombination of discharged H atoms into the molecule.

Graphene, one of the most investigated forms of carbon in recent years, appears to be promising material in design and development of modern electrocatalytic materials[5,6]. In recently published paper[7], authors used combined DFT and experimental study of reduced graphene oxide (rGO) on nickel foam to get insight into the thermodynamics and mechanism of promotion effects of rGO and concluded that reduction persistent oxygen

groups on basal plane (hydroxyl and epoxy) are responsible for HER activity enhancement.

### Experimental details

Graphene oxide films were drop-casted from aqueous-ethanol suspension on clean copper substrate and dried under vacuum. Such prepared GO modified electrodes were immersed in sulfate nickel bath with  $\text{Ni}^{2+}$  at concentration of  $17 \text{ g/dm}^3$  and electrolyzed under potentiostatic as well as galvanostatic regime. Copper substrates without GO film were also electrolyzed in the same manner in order to prepare pure nickel surface as a reference. Also, GO modified copper substrates were electrolyzed in solution of sodium sulfate in order to probe electrocatalytic activity of pure reduced graphene oxide (rGO).

Pseudostationary voltammograms for HER were recorded in Ar-purged 1 M aqueous KOH on pure copper, Ni-modified copper, rGO modified copper and rGO/Ni modified copper.

### Results and discussion

Several features can be observed on pseudostationary linear sweep voltammograms for HER in 1 M KOH on samples obtained by potentiostatic reduction at  $-1.2 \text{ V}$  vs Ag/AgCl reference (**Fig. 1**). Beside expected difference in HER overpotentials for bare copper (Cu) and Ni-coated copper (CuNi), further decrease of overpotential is observed on nickel deposited on GO modified copper substrate. Considering that reduction potential is sufficient for irreversible reduction of GO (as we determined by cyclic voltammetry in nickel-free sodium sulfate solution), and that mass of GO is same for all samples (ca.  $50 \text{ }\mu\text{g}$ ), mass of Ni and hence Ni/rGO ratio was increased by increasing electrolysis time. For thus prepared samples, HER overpotential decreases as electrolysis time increases from 10 up to 60 seconds. Further increase of electrolysis time results in gradual change of trend, which is evident from voltammograms for samples obtained after 150 and 200 seconds of deposition (CuGONi 150 and CuGONi200 in **Fig. 1**). This change of trend can be expected at an intuitive level, as prolonged electrolysis leads to complete coverage of reduced graphene oxide by Ni.

Another interesting feature is the emergence of reduction peak before sharp increase of current density, probably due to the reduction of Ni-hydroxide species formed in KOH. This peak is evident for all rGO/Ni samples, except for the one obtained by shortest electrolysis.

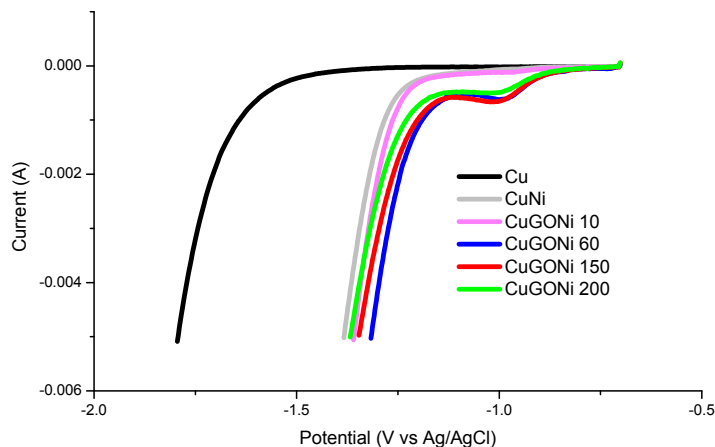


**Fig. 1.** Pseudostationary voltammograms of copper, nickel, and rGO/Ni composites in 1 M KOH. Numbers in legend indicate duration of reduction in nickel bath in seconds.

**Fig. 2.** shows potentials vs. Ag/AgCl reference for two different current densities (1 and 0,1 A dm<sup>-2</sup>) for HER on rGO/Ni samples and pure Ni. It is evident that, in order to maintain specified current density, samples electrolyzed for 60 and 100 seconds achieve highest potentials. Insufficient nickel surface could be responsible for lower activity of samples electrolyzed for 10 and 30 seconds, while drop of the activity for CuGONi 150 and 200 can be ascribed to thick nickel coating that prevents contact of rGO with adsorbed species.

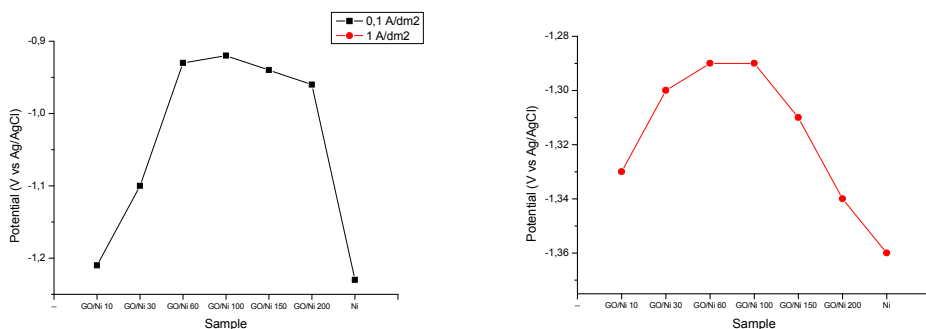


**Fig. 2.** Hydrogen evolution potentials for two different current densities. Numbers in sample names indicate duration of reduction in nickel bath in seconds. Pure nickel deposit was obtained after 30 seconds of electrodeposition.

## Conclusion

Presented results give some insight into the beneficial effect of reduced graphene oxide on the catalytic properties of nickel towards the HER in alkaline electrolyte, which is achieved by controlling the Ni/rGO ratio on the catalytic surface through simple regulation of experimental parameters. Although exact rGO/Ni ratio is not known, it is evident that catalytic activity considerably increase upon electrodeposition of nickel, achieves maximum and decrease for longer Ni deposition times, where rGO become completely covered with nickel, preventing spillover of discharged H atoms and their recombination to H<sub>2</sub>.

## References

- [1] D. Strmcnik *et al.*, Nano Energy, 2016, doi: 10.1016/j.nanoen.2016.04.017.
- [2] W. Sheng, H.A. Gasteiger, Y. Shao-Horn, J. Electrochem. Soc., 2010, **157**, B1529-B1536.
- [3] F. Rößner, Handbook of Heterogenous Catalysis 2nd edition, 2008, **1**, 1574-1585.
- [4] W.C. Conner, Jr., J.L. Falconer, Chem. Rev., 1995, **95**, 759-788.
- [5] D.S. Su, S. Perathoner, and G. Centi, Chem. Rev, 2013, **113**, 5782-5816.
- [6] D. Haag, H.H. Kung, Top. Catal., 2014, **57**, 762-773.
- [7] D. Chanda *et al.*, Phys. Chem. Chem. Phys., 2015, **17**, 26864-26874.

# IMPROVED HER ACTIVITY OF Ni CATHODE ACTIVATED BY NiCoMo IONIC ACTIVATOR – A DFT ASPECT

Dragana D. Vasić Aniđijević, Sladjana Lj. Maslovara, Vladimir M. Nikolić,  
Milica P. Marčeta Kaninski

*Vinča Institute of Nuclear Sciences, University of Belgrade, Mike Alasa 12-14  
Belgrade, Serbia*

## Abstract

We provide some analysis of catalytic activity of nickel electrodes activated by NiCoMo ionic activators for alkaline electrolysis of water, which were studied experimentally in our previous research, leaning on a set of DFT calculations. We propose explanation for partial roles of applied activators, primarily Mo and Co, in modification of intrinsic electrode properties, through analysis of adsorption energetics of water and hydrogen, as well as stability analysis, on appropriate model surfaces.

## Introduction

Nickel cathodes are commonly used in the catalysis of hydrogen evolution in alkaline conditions because of the optimal catalytic activity and satisfactory stability. So far there is a number of studies dealing with the modification of nickel electrodes with Co and Mo to improve the performance of alkaline water electrolysis (for example, see [1]). In our previous work [2] we developed relatively low-cost cathodes with improved performance referred to pure Ni electrodes in the alkaline electrolyser, based on *in situ* electrode activation by (tris(ethylenediamine)Ni(II)chloride tris(ethylenediamine) Co(III) chloride and sodium molybdate – further in text NiCoMo).

In this work we will use density functional theory (DFT) to provide a deeper understanding of fundamental properties of NiCoMo activated electrodes determining their catalytic activity for HER in alkaline media, primarily through investigation of adsorption of hydrogen and water on appropriate NiCoMo model surfaces.

## DFT calculation details

Periodic DFT calculations were performed using PWscf code of the Quantum ESPRESSO distribution [3], with ultrasoft pseudopotentials [4] within GGA-PBE approximation [5]. Kinetic energy cutoff was 25 Ry and charge density cutoff was 250 Ry. Equilibrium lattice constants of Ni and Co were:  $a_{0,Ni} = 3.518\text{\AA}$ ,  $a_{Co} = 2.501\text{\AA}$  and  $c_{Co} = 4.07\text{\AA}$  respectively. Hexagonal  $2 \times 2$  supercells were used in all calculations. Vacuum thickness was at least 12 Å. Dipole correction was used to prevent electrostatic coupling of the periodic images.

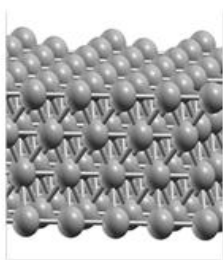
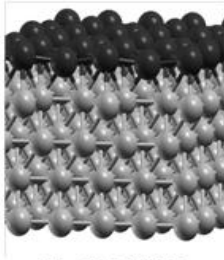
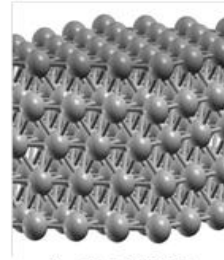
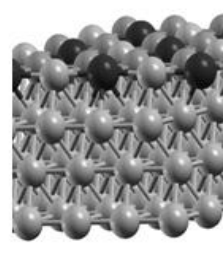
First irreducible Brillouin zone has been sampled by  $4 \times 4 \times 1$  set of k-points grid using Monckhorst-Pack scheme [6]. Bottom two layers were fixed, while all other layers and adsorbate were allowed to relax. Spin polarization was included in all calculations. Differential binding energies (DBE) have been calculated according to a common practice, as in our previous work [7].

## Results and discussion

### *Adsorption of H<sub>2</sub>O and H on NiCoMo model surfaces*

The nickel cathode was modeled as 4 layer Ni slab, while activators were represented by adding an extra surface layer of NiCoMo in variable composition (**Table 1**). Adsorption of H<sub>2</sub>O and H on selected model surfaces has been investigated, as H<sub>2</sub>O and H are key species in Volmer and Heyrovsky steps respectively, and modification of their adsorption properties is expected to exhibit a significant impact on overall reaction rate and mechanism. Adsorption energies are summarized in **Table 1**.

**Table 1.** Adsorption energies of H and H<sub>2</sub>O on investigated model surfaces. Adsorption site is given in parenthesis.

			
<i>Ni(111)</i>	<i>MoML/Ni(111)</i>	<i>CoML/Ni(111)</i>	<i>NiCo2Mo/Ni(111)</i>
<i>E<sub>ads</sub>, H<sub>2</sub>O (adsorption site)</i>			
-0.18 eV (top)	-2.31 eV (dissociated)	-0.21 eV (top)	-1.27 eV (Mo-top dissociated) -0.22 eV (Co-top)
<i>E<sub>ads</sub>, H (adsorption site)</i>			
-2.74 eV (fcc)	-2.64 eV (fcc)	-2.72 eV (fcc)	-2.784 (NiCo2 -fcc)

A strong interaction between Mo atom and oxygen from water is observed, and results in increase of adsorption strength referred to clean Ni(111) from 0.18 eV to at least 1.27 eV, what turned to be enough to provide spontaneous water dissociation on the model surface. When H<sub>2</sub>O is initially adsorbed on Co-top (not preferential) sites in either Co<sub>ML</sub>/Ni(111) or NiCo<sub>2</sub>Mo/Ni(111), no significant changes in adsorption energy referred to clean Ni(111) occur. In all

cases hydrogen adsorption energy varies by less than 0.1 eV, and obtained variations obviously are of limited importance for improvement of HER activity. A proposed key role of Mo in the final effect of improved HER activity can be regarded in light of the consideration of Danilovic *et al.* [8], who pointed to the reactivity for water dissociation as the key property of the materials that show good HER catalytic activity in alkaline media. Increased reactivity towards H<sub>2</sub>O can be further correlated with experimentally observed change of reaction mechanism from Volmer in case of pure Ni to Volmer-Heyrovsky in case of NiCoMo [2]. Volmer step seems to be accelerated upon addition of Mo to the surface, and its rate becomes comparable with the rate of Heyrovsky step, which is mainly dependent on M – H<sub>ads</sub> interaction strength, and hence is not expected to change significantly upon addition of NiCoMo activator.

### ***Estimation of stability trends***

To estimate the stability trends of investigated model surfaces, we calculated differential binding energies (DBE) of Mo and Co atoms in representative systems, and compared them to available data on cohesive energies ( $E_{\text{coh}}$ ) of Co and Mo, according to a common principle [7]: higher DBE referred to  $E_{\text{coh}}$  - better stability is expected. Results are shown in **Table 2**.

**Table 2.** DBE,  $E_{\text{coh}}$  from literature data, and expected stability of Mo and Co atoms in corresponding systems. "\*" refers to values for Co atoms.

<b>System</b>	<b>DBE Mo (Co)</b>	<b><math>E_{\text{coh}}</math> Mo (Co)</b>	<b>stability</b>
<b>Co<sub>ML</sub>/Ni(111)</b>	6.05* eV	4.88* eV [9]	stable
<b>Mo<sub>ML</sub>/Ni(111)</b>	5.26 eV	6.82 eV [10]	unstable
<b>Mo<sub>ML</sub>/Co(111)</b>	4.11 eV	-  -	unstable
<b>NiCo<sub>2</sub>Mo/Ni(111)</b>	6.38 eV	-  -	improved
<b>Ni<sub>2</sub>CoMo/Ni(111)</b>	6.41 eV	-  -	improved
<b>Ni<sub>3</sub>Mo/(Ni111)</b>	6.49 eV	-  -	improved

As expected according to high cohesive energy of Mo, Mo monolayers are unstable on both Ni(111) and Co(111) surfaces. However, Mo in NiCoMo surface alloys promises markedly improved stability referred to Mo monolayers, since its DBE increases. Moreover, stability of Mo in the surface increases with increasing the share of Ni in it, and decreases with share of Co. The role of Co in overall catalytic activity, from the point of view of this stability analysis, might be a matter of Co-Mo co-deposition that tunes stability and amount of Mo, and disables deposition of excess Mo on the surface. As excess Mo is undesirable in the electrode composition, inducing surface destabilization and acting as catalytic poison upon too strong adsorption of water, it is of key importance to keep its content at the optimal level.

## Conclusion

DFT calculated adsorption energies of H and H<sub>2</sub>O on model NiCoMo/Ni(111) surfaces pointed towards the key role of surface Mo in increased reactivity towards water dissociation, thus accelerating Volmer step of HER. Through stability analysis it was shown that Mo monolayer is unstable on Ni(111) surface, although it can be significantly stabilized when its content in the surface is reduced by addition of Ni and Co. Finally it is pointed towards the possibility to control the amount and stability of Mo in the surface, by varying amounts of Ni and Co, which is important when trying to keep Mo content at the optimal level.

## Acknowledgements

The authors would like to thank the Ministry of the Science of the Republic of Serbia for the financial support through Project No. 172045.

## References

- [1] S. Martinez, M. Metikoš-Huković, L. Valek, *Jour Mol Catal A*, 1996, **245** 1-2, 114.
- [2] S. Maslovara, M. Marčeta-Kaninski, I. Perović, V. Nikolić, *Int Jour Hydrogen Energy* 2013, **38** 36, 15928.
- [3] P. Giannozzi, S. Baroni, N. Bonini, M. Calandra, R. Car *et al.*, *J. Phys.: Condens. Matter.*, 2009, **21**, 395502.
- [4] D. Vanderbilt, *Phys. Rev. B*, 1990, **41**, 7892.
- [5] J. P. Perdew, K. Burke, M. Ernzerhof, *Phys. Rev. Lett.*, 1996, **77**, 3865.
- [6] H. J. Monkhorst, J. D. Pack, *Phys. Rev. B*, 1976, **13**, 5188.
- [7] D. D. Vasić, I. A. Pašti, S. V. Mentus, 2013, **38** 12, 5009.
- [8] N. Danilovic, R. Subbaraman, D. Strmcnik, V. R. Stamenkovic and N. M. Markovic, *J. Serb. Chem. Soc.*, 2013, **78** 12, 2007.
- [9] P. H. T. Philipsen, E. J. Baerends, *Phys Rev B*, 1996, **54** 8, 5326.
- [10] C. Kittel, *Introduction to Solid State Physics*, Hoboken, NJ: John Wiley & Sons, Inc, 2005.



# THE ROLE OF METAL IMPURITIES IN THE ELECTROCATALYTIC PERFORMANCE OF NITROGEN-DOPED CARBON MATERIAL

Urša Petek<sup>1,2</sup>, Francisco Ruiz-Zepeda<sup>1</sup>, Martin Šala<sup>1</sup>, Primož Jovanovič<sup>1</sup>,  
Jonas Pampel<sup>3</sup>, Tim Patrick Fellinger<sup>3</sup>, Vid Simon Šelih<sup>1</sup>, Marjan Bele<sup>1</sup>,  
Miran Gaberšček<sup>1,2</sup>

<sup>1</sup>National Institute of Chemistry, Hajdrihova 19, Ljubljana, Slovenia; <sup>2</sup>Faculty of Chemistry and Chemical Technology, Večna pot 113, Ljubljana, Slovenia;  
<sup>3</sup>Department of Colloid Chemistry, Max Planck Institute of Colloids and Interfaces, Am Mühlenberg 1, Potsdam, Germany

In fuel-cell electrocatalysis, there is a demand for effective low-cost alternatives to Pt- based catalysts for oxygen reduction reaction (ORR). A well studied group of non-noble catalysts are metal-free nitrogen-modified carbon materials, which are reported to be efficient electrocatalysts in alkaline electrolytes [1]. Some synthetic procedures to prepare N-doped carbons include steps that can lead to metal contamination of the material. It has been suggested that even small amounts of residual metal impurities could have an effect on the observed electrocatalytic activity of the material [2,3].

We studied the role of residual metals in a N-doped carbon material that was prepared by ionothermal synthesis adapted from ref. [4]. Adenine was carbonized in a melt of KCl and ZnCl<sub>2</sub> in alumina crucibles. The resulting N-doped carbon contained residual Zn and Al. Distribution of metals in the material was examined under aberration-corrected scanning transmission electron microscope. Electrochemical stability of the metals was examined in an electrochemical flow cell coupled to inductively coupled plasma mass spectrometer. Electrocatalytic activity of the material was studied using the rotating disc electrode method.

## References

- [1] H.W. Liang, X. Zhuang, S. Brüller, X. Feng, K. Müllen, Nat. Commun., 2014, **5**, 4973.
- [2] L. Wang, M. Pumera, Chem. Commun., 2014, **50**, 12662-12664.
- [3] J. Masa, W. Xia, M. Muhler, W. Schuhmann, Angew. Chem. Int. Ed., 2015, **54**, 10102-10120.
- [4] J. Pampel, T.P. Fellinger, Adv. Energy Mater., 2016, **6**, 1502389.

## FROM GREEN SOLVENT TO CARBON MATERIAL: APPLICATION OF IONIC LIQUID DERIVED CARBON FOR OXYGEN REDUCTION

Nikola Zdolšek<sup>1</sup>, Aleksandra Dimitrijević<sup>1</sup>, Tatjana Trtić-Petrović<sup>1</sup>,  
Jugoslav Krstić<sup>3</sup>, Danica Bajuk-Bogdanović<sup>2</sup>, Biljana Šljukić<sup>2</sup>

<sup>1</sup>Laboratory of Physics, Vinča Institute of Nuclear Sciences, University of Belgrade, Mike Petrovića Alasa 12 – 14, 1101 Belgrade, Serbia; <sup>2</sup>Faculty of Physical Chemistry, University of Belgrade, Studentski trg 12–16, 11158 Belgrade, Serbia; <sup>3</sup>University of Belgrade, IChTM, Njegoševa 12, 11000 Belgrade, Serbia

Oxygen reduction reaction (ORR) is an important process in energy conversion systems such as fuel cells and lithium – air batteries, in gas sensors and in the electrosynthesis of hydrogen peroxide [1]. In the present work two carbon materials based on ionic liquid were investigated as electrocatalysts for the ORR. 1-butyl-3-methylimidazolium methane sulfonate was used as the medium for the conversion of glucose precursor into porous carbon in the ionothermal synthesis and as a precursor for sulfur-doped porous carbon in the direct carbonization of ionic liquid. The synthesized carbon materials were characterized by SEM, EDS, Raman spectroscopy and N<sub>2</sub> physisorption at 77K.

To investigate the electrocatalytic activity of the synthesized carbon materials for the ORR, cyclic voltammetry experiments were performed in 0.1 M KOH solution saturated with N<sub>2</sub> or O<sub>2</sub>. Electrode based on direct carbonization of ionic liquid gave cathodic peak at lower overpotential (peak at 0.6 V vs. RHE). Additional electrochemical characterization was done by linear sweep voltammetry with a rotating disk electrode. The results showed that direct carbonization of 1-butyl-3-methylimidazolium methane sulfonate ionic liquid gave carbon doped with sulphur and with very good characteristic for application for ORR with direct four electron pathway mechanism. Contrary, ionothermal carbon showed lower electrocatalytic activity with two – step two – electron pathway.

### References

[1] B. Šljukić, C. E. Banks, R. G. Compton, J. Iran. Chem. Soc., 2005, **2**, 1–25.

## INFLUENCE OF NON-AQUEOUS SOLVENTS ON ORR ELECTROCHEMISTRY

Nemanja Gavrilov, Miloš Stevanović, Igor A. Pašti, Slavko V. Mentus

*University of Belgrade, Faculty of Physical Chemistry, Studentski trg 12-16, 11158  
Belgrade, Serbia*

Harnessing substantial portion of the theoretical specific energy in Li-air batteries, exciting by  $\sim 100$  fold that of Li-ion, is the driving force for the development of new energy storage devices. Still, operating the battery for numerous cycles efficiently, stably and sustainably remains a daunting challenge. Understanding the electrochemical mechanism of  $O_2$  reduction at the cathode in  $Li^+$  containing aprotic electrolytes can be crucial in overcoming part of the problem [1]. Herein we used cyclic voltammetry to elucidate the ORR mechanism and kinetics in four different solvents, namely, dimethyl sulfoxide (DMSO), acetonitrile (MeCN), dimethylformamide (DMF) and propylene carbonate (PC), possessing a range of properties with tetrabutylammonium hexafluorophosphate (TBAPF<sub>6</sub>) or lithium hexafluorophosphate (LiPF<sub>6</sub>) electrolyte solution. By comparing CVs it is evident that the solvent and the supporting electrolyte act complementary to influence the nature of the reaction products and in turn ORR mechanism. Results show that the interaction of a small, highly charged  $Li^+$  with surrounding solvent and counter ions is markedly different than large, bulky TBA<sup>+</sup> ion and such interactions strongly affect the reaction mechanism of oxygen reduction and oxygen mobility through the electrolytes, which is in line with literature [2]. Furthermore, the differences seen in the reversibility of the ORR in TBA<sup>+</sup> compared to  $Li^+$  containing electrolytes is probably due to the formation of insulating  $Li_2O$  or  $Li_2O_2$  on the cathode during discharge process that is clearly discernible as the downshift or the absence of the return peak in CVs. Full understanding of the mechanism of ORR in aprotic electrolytes will enable further development in Li-air technology and electrolyte selection which will further improve their efficiency.

### References

- [1] J. Scheers, D. Lidberg, K. Sodeyama, Z. Futerab and Y. Tateyama, *Phys. Chem. Chem. Phys.*, 2016, **18**, 9961-9968.
- [2] L. Johnson, C. Li, Z. Liu, Y. Chen, S.A. Freunberger, P.C. Ashok, B.B. Praveen, K. Dholakia, J.M. Tarascon, P.G. Bruce, *Nat Chem.*, 2014, **6**, 1091-1099.

# Pt-ALLOY ELECTROCATALYSTS FOR THE OXYGEN REDUCTION REACTION: FROM MODEL SURFACES TO NANOSTRUCTURED SYSTEMS

Viktor Čolić<sup>1</sup>, Aliaksandr Bandarenka<sup>1,2</sup>

<sup>1</sup>Physics of Energy Conversion and Storage - ECS, Physik-Department, Technische Universität München, James-Frank-Straße 1, 85748 Garching, Germany;

<sup>2</sup>Nanosystems Initiative Munich (NIM), Schellingstraße 4, 80799 Munich, Germany

The slow rate of the cathodic oxygen reduction reaction (ORR) is one of the main factors hindering the more widespread implementation of polymer electrolyte membrane fuel cells (PEMFCs). In order to improve the kinetics of the ORR, alloys of Pt with late transition metals and lanthanides have been studied extensively, as they potentially offer enhanced activity and reasonable stability. Nonetheless, many of them cannot be considered “model objects” as their surface composition and structure are not stable under operating conditions. Under PEMFC conditions, the “solute” metal can dissolve from the surface and near-surface layers. This process often results in a structure in which several Pt-enriched layers cover the bulk alloy and protect it from further dissolution. In this work [1], we analyze the literature results on the electrocatalytic properties of these alloys, from single crystals and polycrystalline materials to nanoparticles. Given that the formed Pt-rich overlayer is several atomic layers thick, the so-called strain effects should primarily determine the behavior of these catalysts. The strain in the system is, in turn, the result of the difference between the lattice parameters of the alloy and Pt-rich layer. This causes changes in the electronic structure, and, consequently, in the binding properties of the surface. We propose that the atomic radius of the solute metal can be used in some particularly complex systems (*e.g.* polycrystalline and nanostructured alloys) as a simple semi-empirical descriptor, statistically connected to the resulting lattice strain. The implications of this phenomenon can be used to explain qualitatively the behavior of certain Pt-alloy nanoparticles so far considered “anomalous”.

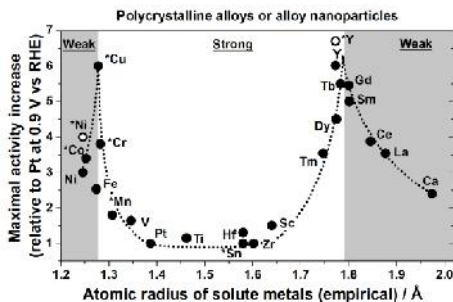


**Fig. 1.** The maximal reported relative activities of Pt-alloy catalysts towards the ORR, at 0.9 V vs. RHE, in comparison to the corresponding Pt-catalyst, plotted versus the empirical radius of the solute metal. The asterisks denote nanoparticles. Grey are - weak binding, white area - strong binding of the intermediates.

***Electrocatalyst stability/  
DURAPEM session***

---



## HOW TO IMPROVE THE STABILITY OF PLATINUM-BASED ELECTROCATALYSTS?

A. Pavlišič<sup>1,2</sup>, P. Jovanovič<sup>2</sup>, V. S. Šelih<sup>2</sup>, M. Šala<sup>2</sup>, M. Bele<sup>2</sup>, G. Dražić<sup>2</sup>, I. Arčon<sup>3</sup>, S. Hočevar<sup>2</sup>, A. Kokalj<sup>4</sup>, N. Hodnik<sup>2</sup>, M. Gaberšček<sup>\*2,1</sup>

<sup>1</sup> Faculty of Chemistry and Chem. Tech., University of Ljubljana, Slovenia;

<sup>2</sup> National Institute of Chemistry, Hajdrihova Ulica 19, Ljubljana, Slovenia;

<sup>3</sup> University of Nova Gorica Vipavska 13, SI-5000, Nova Gorica, Slovenia; <sup>4</sup> Jožef Stefan Institute Jamova 39, 1000 Ljubljana, Slovenia

During the past decade, significant progress has been made in the development of high performance electrocatalysts for potential use in various devices such as electrolyzers, low temperature fuel cells, reverse fuel cells, photocatalysts etc. A very promising direction has been alloying of platinum with transition elements, X, to obtain bimetallic alloys of PtX (X=Ni, Co, Ru, Cu etc). Namely, when in contact with platinum, transition metals can extremely enhance the rate of electrochemical reaction, due to the so-called d-band center shift, ligand effect and similar electronic phenomena. However, at the same time the presence of less noble metals considerably enhances the degradation of catalyst. We will present various degradation phenomena in pure and alloyed electrocatalysts [1] - under realistic conditions found in electrocatalytic devices - and show directions towards improvement of their stability.



**Fig. 1.** Activity vs. stability: a dichotomy to be resolved in alloy-based electrocatalysts.

### References

[1] A. Pavlisic *et al.*, ACS Catal., 2016, **6**, 5530-5534.

## ADVANCED CHARACTERIZATION ELECTROCHEMICAL METHODS FOR STUDYING NANOPARTICLE ELECTROCATALYSTS STABILITY

Nejc Hodnik\*, Primož Jovanovič, Matija Gatalo, Francisco Ruiz-Zepeda,  
Marjan Bele, Miran Gaberšček

*National Institute of Chemistry, Hajdrihova 19, 1000 Ljubljana, Slovenia  
(\*[nejc.hodnik@ki.si](mailto:nejc.hodnik@ki.si))*

Electrocatalysis plays a crucial role in the future green and sustainable energy infrastructure. Energy conversion, which is envisioned to act as a buffer for mismatch between energy demand and supply of intermittent energy sources from wind and sun, incorporates water cycle based devices such as proton exchange membrane fuel cells and electrolyzers that contain precious metals like platinum and iridium. On one side, these metals are expensive and potentially limited in the supply whereas on the other they are prone to stability issues. Both facts mentioned hinder the commercialization of these devices and thus drive the scientific efforts towards reduction of metal loadings and increase of its performance or even its replacement, which at this moment is still not a realistic scenario.

For the purposes of studying and understanding of degradation mechanisms like metal dissolution/leaching, carbon corrosion, particle agglomeration/coalescence, etc., we have utilized and also developed advanced characterization electrochemical methods, such as identical location electron microscopy [2,3], in-situ electrochemical liquid TEM, electrochemical cell coupled to ICP-MS [3,4], etc.

### References

- [1] N. M. Markovic, Nat. Mater., 2013, **12**, 101–102.
- [2] N. Hodnik, J. Phys. Chem. C, 2012, **116**, 21326–21333.
- [3] N. Hodnik, J. Phys. Chem. C, 2015, **119**, 10140–10147.
- [4] P. Jovanovič, J. Power Sources, 2016, just accepted.



# ELECTROCATALYSTS STABILITY INVESTIGATION BY ELECTROCHEMICAL FLOW CELL ANALYTICS

Primož Jovanovič<sup>1</sup>, Andraž Pavlišič<sup>1</sup>, Vid Simon Šelih<sup>2</sup>, Martin Šala<sup>2</sup>, Samo Hočevár<sup>2</sup>,  
Marjan Bele<sup>1</sup>, Francisco Ruiz-Zepeda<sup>1</sup>, Goran Dražić<sup>1</sup>, Nejc Hodnik<sup>3</sup>,  
Miran Gaberšček<sup>1,4</sup>

*<sup>1</sup>Department of Materials Chemistry, National Institute of Chemistry, Hajdrihova 19, SI-1000 Ljubljana, Slovenija, <sup>2</sup>Department of Analytical Chemistry, National Institute of Chemistry, Hajdrihova 19, SI-1000 Ljubljana, Slovenija, <sup>3</sup>Department of Catalysis and Chemical Reaction Engineering, National Institute of Chemistry, Hajdrihova 19, SI-1000 Ljubljana, Slovenija, <sup>4</sup>Faculty of Chemistry and Chemical Technology, University of Ljubljana, Večna pot 113, SI-1000 Ljubljana, Slovenija*

Electrocatalysts play an important role in sustainable energy-related fields. As these catalysts still need improvement on activity and especially stability, a lot of effort is invested in developing new materials. However, their application is hindered due to the complex interplay of different parameters. A more rapid development of electrocatalysts can be achieved with the help of advanced experimental tools [1]. To tackle this, an electrochemical flow cell (EFC) linked to inductively coupled plasma mass spectrometer (ICP-MS) has been utilized for catalyst stability research. The applicability of the method will be demonstrated on a few dissolution studies of nanoparticulate electrocatalysts for proton exchange membrane fuel cells and electrolyzers.

## References

[1] S. Mezzavilla, S. Cherevko, C. Baldizzone, E. Pizzutilo, G. Polymeros, K.J.J. Mayrhofer, ChemElectroChem., 2016, doi:10.1002/celc.201600170.

## TUNING THE STABILITY OF PtCu<sub>3</sub>/C ORR ELECTROCATALYST WITH GOLD DECORATION AND GOLD DOPING

Matija Gatalo<sup>1\*</sup>, Primož Jovanovič<sup>1</sup>, Jan-Philipp Grote<sup>2</sup>, Francisco Ruiz-Zepeda<sup>1</sup>,  
Nejc Hodnik<sup>1</sup>, Goran Dražič<sup>1</sup>, Marjan Bele<sup>1</sup>, Karl J.J. Mayrhofer<sup>2,3</sup>,  
Miran Gaberšček<sup>1</sup>

<sup>1</sup>National Institute of Chemistry, Hajdrihova 19, SI-1000 Ljubljana, Slovenia; <sup>2</sup>Max-Planck-Institut für Eisenforschung GmbH, Max-Planck Str. 1, 40237 Düsseldorf, Germany; <sup>3</sup>Helmholtz-Institut Erlangen-Nürnberg (HI ERN), Nögelsbachstr. 49 b, 91052 Erlangen, Germany (\*[Matija.gatalo@ki.si](mailto:Matija.gatalo@ki.si))

Carbon supported Pt alloy electrocatalysts are not stable during proton exchange membrane (PEM) fuel cell operating conditions. We hereby present an effective strategy of about 1% atomic gold addition to a PtCu<sub>3</sub>/C oxygen reduction reaction (ORR) electrocatalyst that reduces the rate of two key degradation mechanisms – corrosion of carbon support and removal of less noble metal without any trade-off in ORR activity.[1] The addition of gold results in either gold decoration or gold doping of the PtCu<sub>3</sub>/C ORR electrocatalyst. Decoration with gold is achieved through galvanic displacement of superficial copper found on selected spots on the PtCu<sub>3</sub> nanoparticles surface with gold precursor salt, while gold doping is achieved by subsequent thermal annealing of gold decorated PtCu<sub>3</sub>/C electrocatalyst.

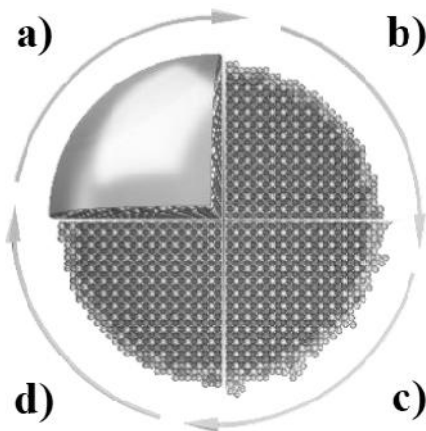


**Fig. 1.** (a) Model of an ordered PtCu<sub>3</sub> nanoparticle with (b) Pt surface segregation, (c) gold decoration and (d) gold doping.

# FIRST PRINCIPLES INSIGHTS INTO GRAPHENE ELECTRONIC AND CHEMICAL PROPERTIES MODIFICATION BY SUBSTITUTIONAL DOPING

Ana S. Dobrota\*, Igor A. Pašti

*University of Belgrade, Faculty of Physical Chemistry, Studentski trg 12-16, 11158  
Belgrade, Serbia (\*[ana.dobrota@ffh.bg.ac.rs](mailto:ana.dobrota@ffh.bg.ac.rs))*

Since its experimental discovery, graphene's fascinating properties have placed it in the focus of the Materials Science research community, to be considered for many possible applications. The presence of various types of defects in graphene alters its electronic properties and consequently, its reactivity. Such modifications open up additional possibilities for graphene applications, including fuel cells, in which graphene can be used as the oxygen reduction catalyst, or as a catalyst support. Oxygen functional groups are often present in carbonaceous materials, and can promote the degradation of the catalyst and/or the carbon support and affect the fuel cell's performance. Substitutional doping is the standard method for controlling the semiconducting properties in conventional, inorganic semiconductors. When it comes to graphene, boron and nitrogen atoms are natural candidates for doping due to their similar atomic size as that of carbon. The effects of substitutional doping of graphene with B, N, P and S on the reactivity of the graphene basal plane were investigated systematically, using Density Functional Theory calculations. The OH adsorption on vacant and substitutionally doped graphene, as well as on their oxidized forms, was analyzed and compared to the case of OH adsorption on pristine graphene. H adsorption on these models was also investigated, in order to establish a link between the electronic structure of defected graphene and its reactivity towards H and OH, which could participate in painting a universal picture of the reactivity trends of the graphene basal plane [1]. The importance of including these groups when modelling doped graphene materials was demonstrated on the example of molecular oxygen adsorption on oxidized and non-oxidized forms of doped graphene. Their inclusion was found to significantly change theoretical results such as adsorption energies, which can be of interest for various applications.

## References

[1] A.S. Dobrota, I.A. Pašti, S.V. Mentus, N.V. Skorodumova, Phys. Chem. Chem. Phys., 2016, **18**(9), 6580-6586.

# INVESTIGATION OF THE RADIOLITICALLY SYNTHESIZED Ag/C CATALYST AS A POTENTIAL CATHODE MATERIAL OF AN ALKALINE FUEL CELL USING NEWLY DESIGNED GAS-FLOW HALF-CELL

Ivan Stoševski<sup>1</sup>, Jelena Krstić<sup>2</sup>, Zorica Kačarević-Popović<sup>2</sup>, Šćepan Miljanić<sup>1,\*</sup>

<sup>1</sup>University of Belgrade, Faculty of Physical Chemistry, P.O. Box 47, 11158 Belgrade 118 PAC 105305, Serbia; <sup>2</sup>University of Belgrade – Vinča Institute of Nuclear Sciences, POB 522, 11001 Belgrade, Serbia ([\\*epan@ffh.bg.ac.rs](mailto:epan@ffh.bg.ac.rs))

In our previous work [1] carbon supported silver nanoparticles (Ag/C) synthesized by gamma irradiation method were characterized and investigated as electrocatalysts for oxygen reduction reaction (ORR) in an alkaline medium. Electrochemical measurements, such as cyclic voltammetry, were conducted in the standard three electrode electrochemical cell with the rotating working disc electrode. Here, we further investigate the catalyst capability for application in an alkaline fuel cell using an in-house fabricated three electrode gas flow half-cell. The half-cell is specially designed to simulate the operating conditions and environment of a fuel cell at the working electrode. The working electrode consists of the Ag/C catalyst deposited on a hydrofobized carbon paper (Toray 35BC) and it is in a direct contact with a PVA/KOH matrix membrane [2]. On the other side of the membrane there is 2 M KOH electrolyte, with reference and counter electrodes immersed in.

The chemical composition and loading of Ag/C based catalytic layer was optimized by preparing different layers and investigating their activities for ORR. The best performed Ag electrode was compared with the commercial platinum one (Fuel Cells Etc). It operates at 100-150 mV higher overpotentials, as expected [3]. The half-cell was further used to predict a performance (e.g. polarization curves and power densities) of the fuel cell with a silver based cathode and the one with Pt based cathode. The polarization curve has been simulated by recording polarization curves for both the ORR and hydrogen oxidation reaction. The fuel cell with Ag/C based cathode has shown four times less specific power density than one with a platinum cathode. Taking into account that the price of silver is approximately 1/60 of the platinum price, it can be concluded that radiolitically synthesized Ag/C catalyst provides a good foundation for application in an alkaline fuel cell. Furthermore, the half-cell has the potential to simplify and speed up research testing in fuel cells as it enables faster and more reliable measurements with spending less material than in a standard fuel cell testing.

## References

- [1] I. Stoševski, J. Krstić, J. Milikić, B. Šljukić, Z. Kačarević-Popović, S. Mentus, Š. Miljanić, *Energy*, 2016, **101**, 79–90.
- [2] I. Stoševski, J. Krstić, N. Vokić, M. Radosavljević, Z.K. Popović, Š. Miljanić, *Energy*, 2015, **90**, 595–604.
- [3] J.S. Spendelow, A. Wieckowski, *Phys. Chem. Chem. Phys.*, 2007, **9**, 2654–2675.

Organization of the meeting was supported by ANALYSIS d.o.o.

# Sve za Vašu laboratoriju na jednom mestu

**ATAGO**  
Refraktometri i polarimetri

**EHRET**  
Lutirna i biološka komore i izolatori

**Thermo SCIENTIFIC**  
Analitička oprema: F-HR i F-HR, F-HR, Raman, UV/VIS, HPLC, IC, GC, GC-MS, ICP, ICP-MS, HRRS, AAS, ICP, ICP-MS, TOC, TS, TNCX, DES, XRF, NMR, (Serijske opreme): Inkubatori, Vakuumirani, i hlađe...

**WALDNER Firmengruppe**  
Laboratorijske nameštaje i digestori

**SOTAX**  
Oprema za titrimetrijske testove i analize tečnosti i kvalitativne analize

**FEDEGARI AUTOKLAVEN**  
Laboratorijski autoklav-parni sterilizatori

**GE**  
IUC

**Riebesam**  
Mašine za pranje dezinfekciju laboratorijalnih posuda i delova

**KERN**  
Vage i legovi

**Retsch**  
Mlinovi i sejalice

**BERGHOF**  
Ploče za digestiju

**BIOSCAPE**  
Kliver i ventilaciona oprema za zbiranje i analizu

**LANGE**  
Laboratorijske i proizvodne upotrebe u analizi vode

**ANALYSIS LABORATORY EQUIPMENT**

**ANALYSIS d.o.o.**  
Gandijeva 76a, 11070 Novi Beograd; Tel/fax: +381-(0)-11-318-64-46; +381-(0)-11-318-64-48  
e-mail: info@analysis.rs; www.analysis.rs